KATHOLIEKE UNIVERSITEIT LEUVEN

thermo research group

New directions in phase-field modeling of microstructure evolution in polycrystalline and multi-component alloys

Nele Moelans

K.U. Leuven, Belgium

School on Computational Modeling of Materials, Antwerp, Dec 2-3, 2010

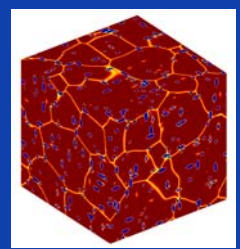

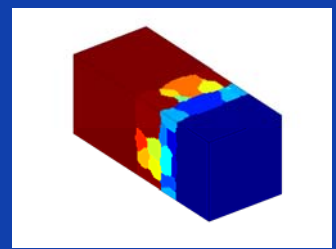

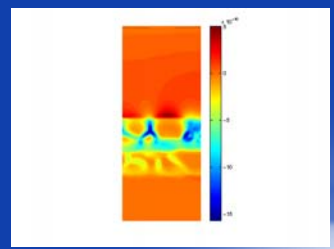

Current state of phase-field modeling

- **Modeling of microstructure evolution**
  - Meso- & micro scale (nm - mm)
  - Based on thermodynamic principles
- **Growing field since 20 years; current topics**
  - Quantitative aspects
  - Realistic, complex, multi component systems
- **Wide field of applications**
  - Solidification, phase transitions, diffusion, grain growth, deformation, crack formation, ferro-electric/magnetic domains, ….

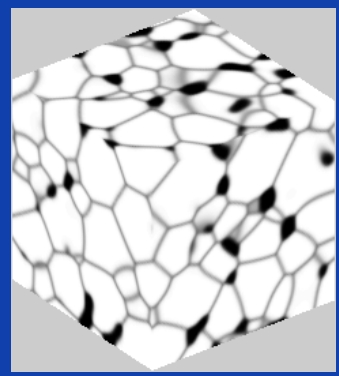

Bulk grain structures

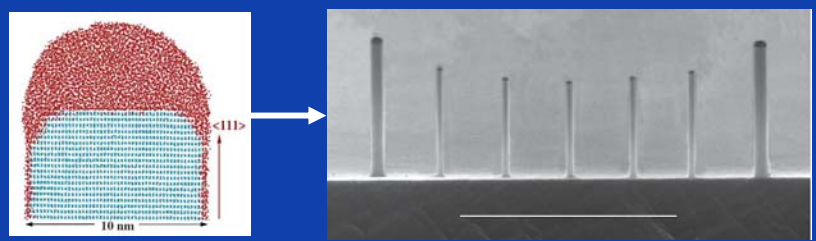

Synergetic growth of nanowires

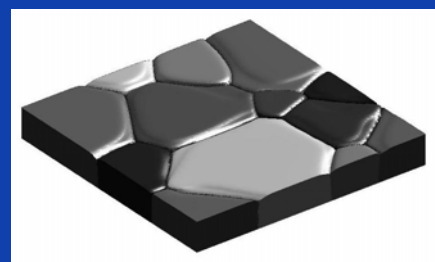

Thin films

KATHOLIEKE UNIVERSITEIT LEUVEN

'Quantitative' phase-field models

- Properties bulk and interfaces are reproduced accurately in the simulations
  - Effect model description and parameters
  - Numerical issues
- => Insights in the evolution of complex morphologies and grain assemblies
  - Effect of individual bulk and interface properties
- Predictive ?
  - Depends on availability and accuracy of input data
    - Requires composition and orientation dependence

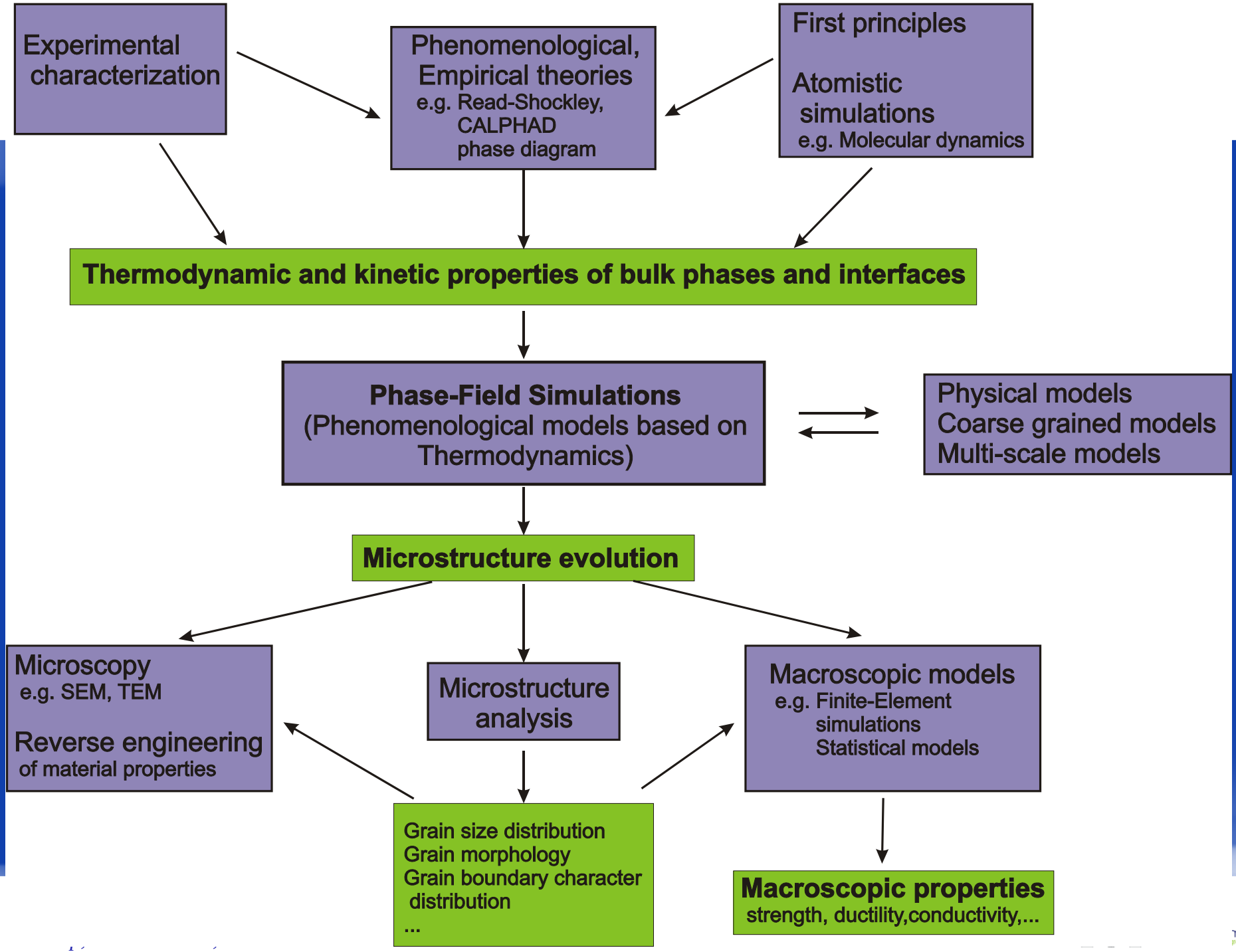
Experimental characterization
Phenomenological, Empirical theories
e.g. Read-Shockley, CALPHAD phase diagram
First principles
Atomistic simulations
e.g. Molecular dynamics
Thermodynamic and kinetic properties of bulk phases and interfaces
Phase-Field Simulations
(Phenomenological models based on Thermodynamics)
Physical models
Coarse grained models
Multi-scale models
Microstructure evolution
Microscopy
e.g. SEM, TEM
Reverse engineering
of material properties
Microstructure analysis
Macroscopic models
e.g. Finite-Element simulations
Statistical models
Grain size distribution
Grain morphology
Grain boundary character distribution
...
Macroscopic properties
strength, ductility,conductivity,...

KATHOLIEKE UNIVERSITEIT LEUVEN

Parameter assessment

- Different kinds of input data
  - Bulk phase stabilities, bulk phase diagram information
    - CALPHAD
  - Interfacial energy and mobility
  - Elastic properties, crystal structure, lattice parameters
  - Diffusion mobilities/coefficients
    - DICTRA mobilities
- Orientation and composition dependence
  - Anisotropy, segregation, solute drag
  - Very important for microstructure evolution, but difficult to measure/calculate

KATHOLIEKE UNIVERSITEIT LEUVEN

Outline

- CALPHAD (CALculation of PHAse Diagrams) – method
- Quantitative phase-field model for multi-phase systems
- Coupling phase-field with thermodynamic databases, example for Ag-Cu-Sn
- Application examples
  - Diffusion controlled growth in Cu/Cu-Sn solder joints

KATHOLIEKE UNIVERSITEIT LEUVEN

thermo research group

CALPHAD (CALculation of PHAse Diagrams) – method

- *Computational thermodynamics: The Calphad Method, H.L. Lukas, S.G. Fries and B. Sundman, Cambridge 2007, ISBN 978-0-521-86811-2*
- *Thermo-Calc : www.thermocalc.se*
- *Calphad : www.calphad.org*

What ?

- **Phase diagrams and thermodynamic Gibbs energies are combined**

Phase diagram

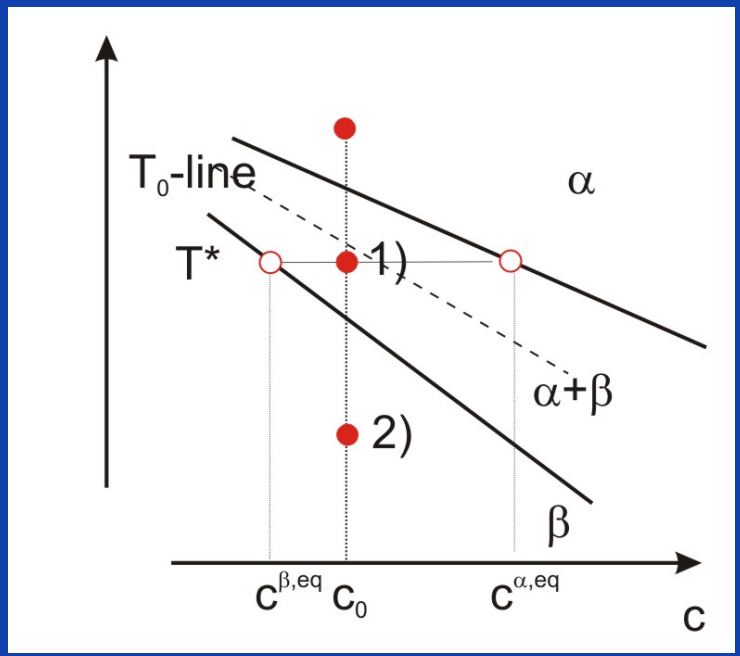

Free energies

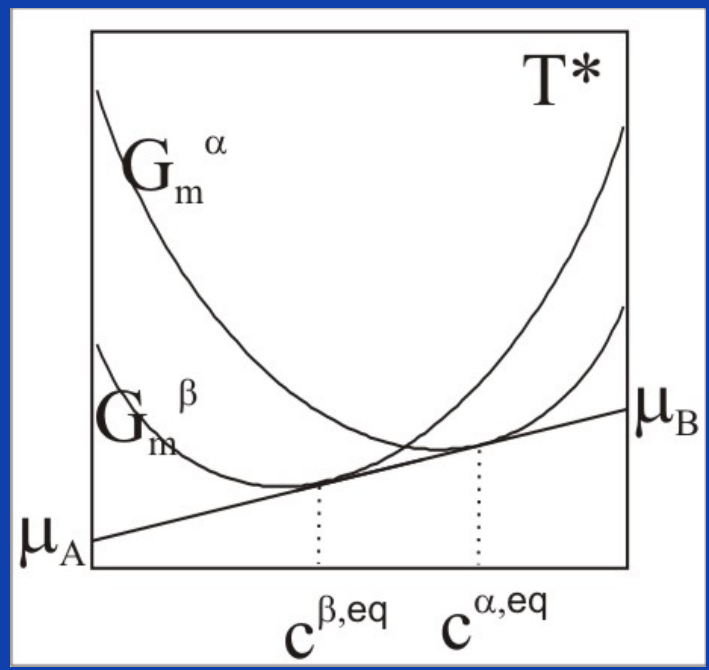

- **Mission: develop a technique for calculating/predicting phase diagrams for multi-component multi-phase materials**

KATHOLIEKE UNIVERSITEIT LEUVEN

What ?

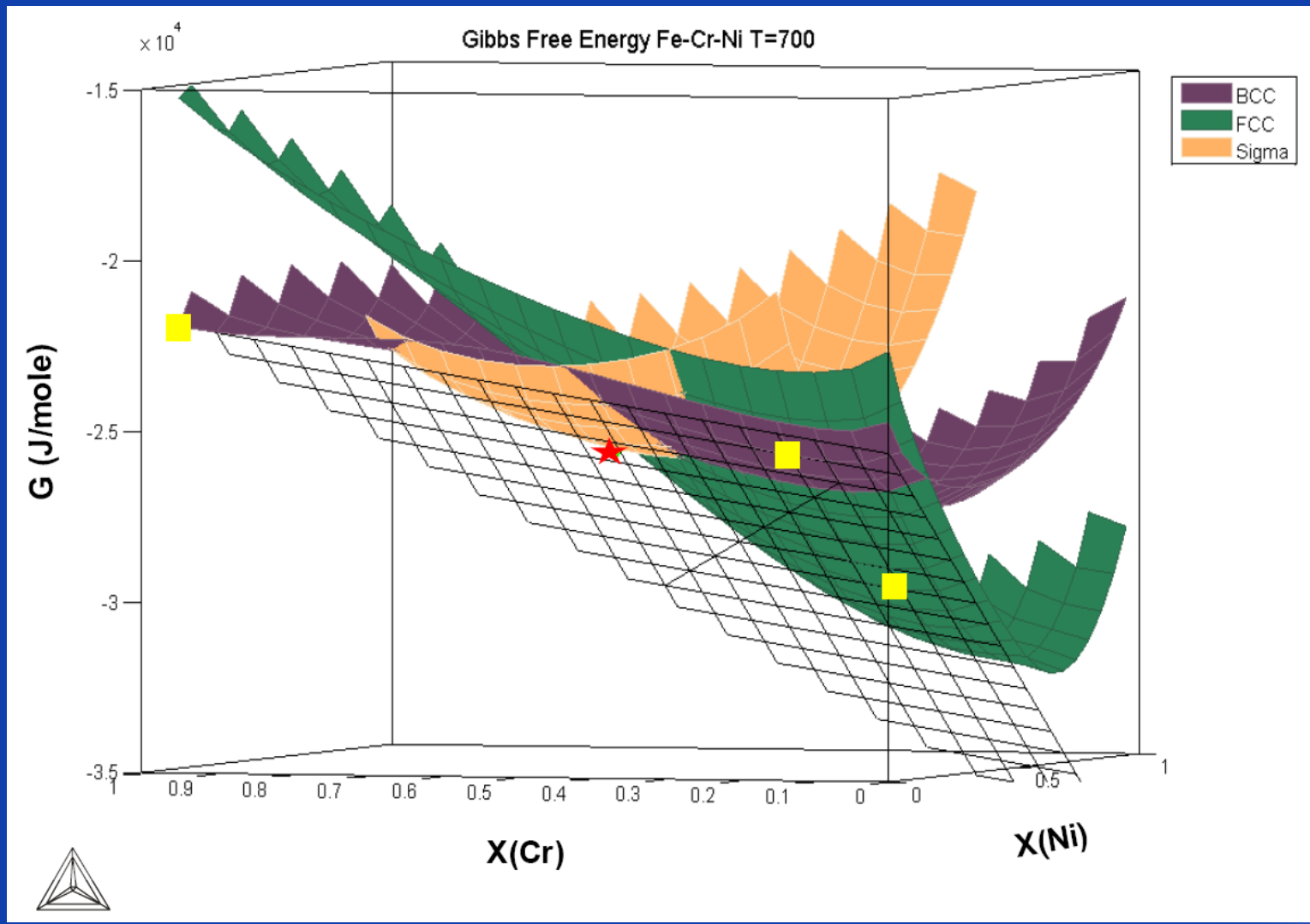

KATHOLIEKE UNIVERSITEIT LEUVEN

What ?

- **STEP 1: Determine G(T,p,x) expressions for all phases**
  - Choice of a thermodynamic model
  - Determination of the parameters based on experimental and theoretical (a.o. ab-initio) input,
    - Such as phase equilibria, heat of formation, vapor pressures, ….
- **STEP 2: Minimization of the total Gibbs energy of a multi-phase system**
  - → Phase diagrams
  - → Thermodynamic quantities: chemical potential, heat of transformation, reaction, …
  - → Input for diffusion and microstructure simulations

KATHOLIEKE UNIVERSITEIT LEUVEN

Pyramidal approach

- E.g. Gibbs energies for ternary system
  - Pure elements, Al, Mg, Si
  - Binary systems, Al-Mg, Al-Si, Mg-Si
  - Ternary system, Al-Mg-Si

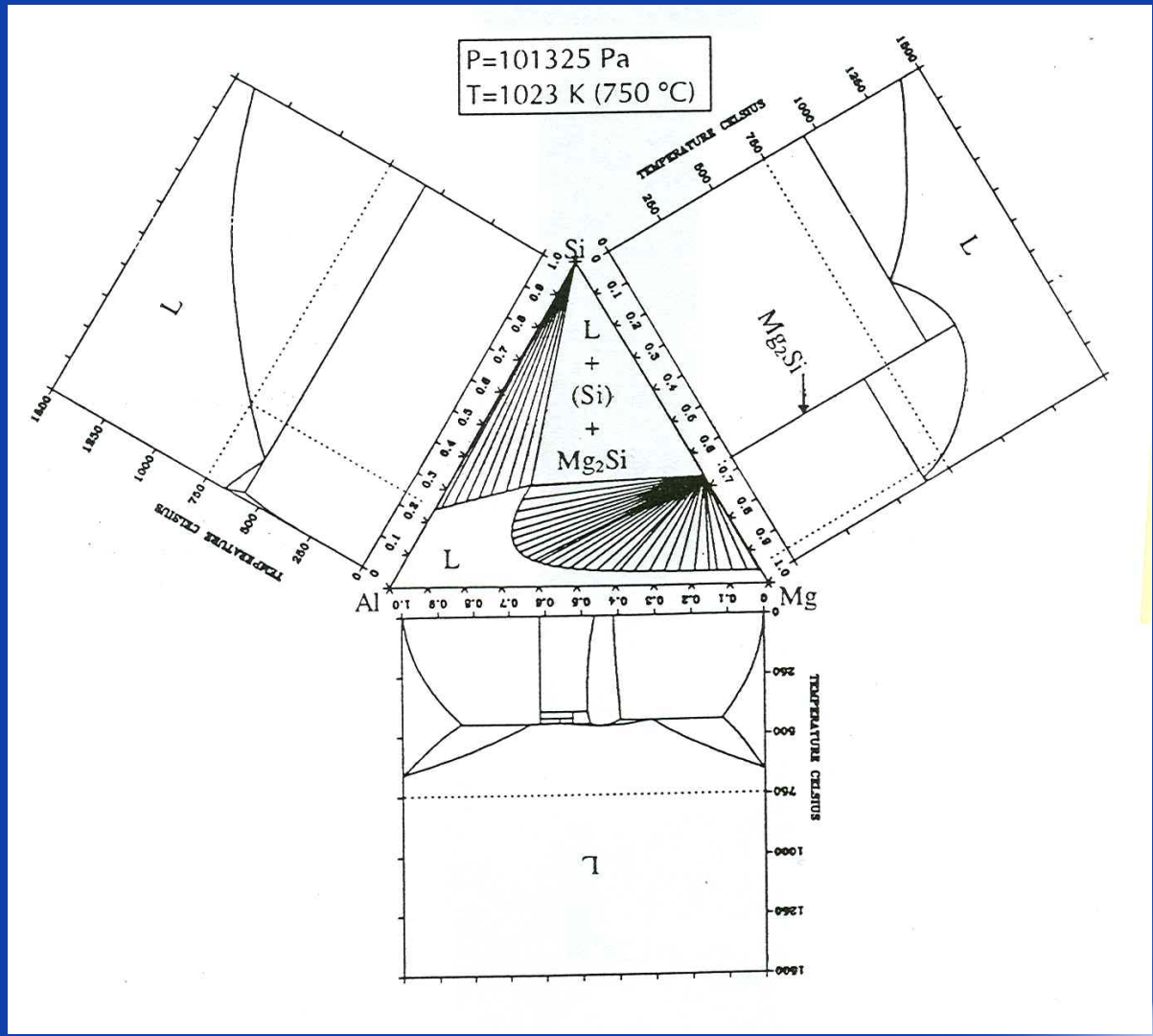

Pure elements

- **Choice of a standard element reference state (SER) for each element (reference structure, temperature and pressure)**

- **Temperature dependence Gibbs energy**

$$G - HSER = a + bT + cT\ln(T) + dT^2 + e\frac{1}{T} + fT^3$$

$$\Rightarrow C_p = -c - 2dT - 2e\frac{1}{T^2} - 6fT^2 + \ldots$$

  - ***a,b,c,d,…* fitted to experiments, ab-initio data**

- **Also models for magnetic ordering, effect of pressure**

Binary substitutional alloys

- **General expression** $G - G^{ref} = G^{id} + G^{ex} + G^{phys}$
  - **Mechanical mixing of pure elements** $G^{ref,\alpha} = x_A G_A^{0,\alpha} + x_B G_B^{0,\alpha}$
  - **Ideal mixing (Raoults solution)** $G^{id} = x_A \ln(x_A) + x_B \ln(x_B)$
  - **Redlich-Kister expression for excess interactions** $G^{ex,\alpha} = x_A x_B L^{\nu}_{AB} (x_A - x_B)^{\nu}$
    - **T-dependenc of L_{AB}^{ν}**

$$L^{\nu}_{AB} = a + bT + cT\ln(T) + dT^2 + e\frac{1}{T} + fT^3$$

    - **L_{AB}^{ν} from experiments**

Regular solution model

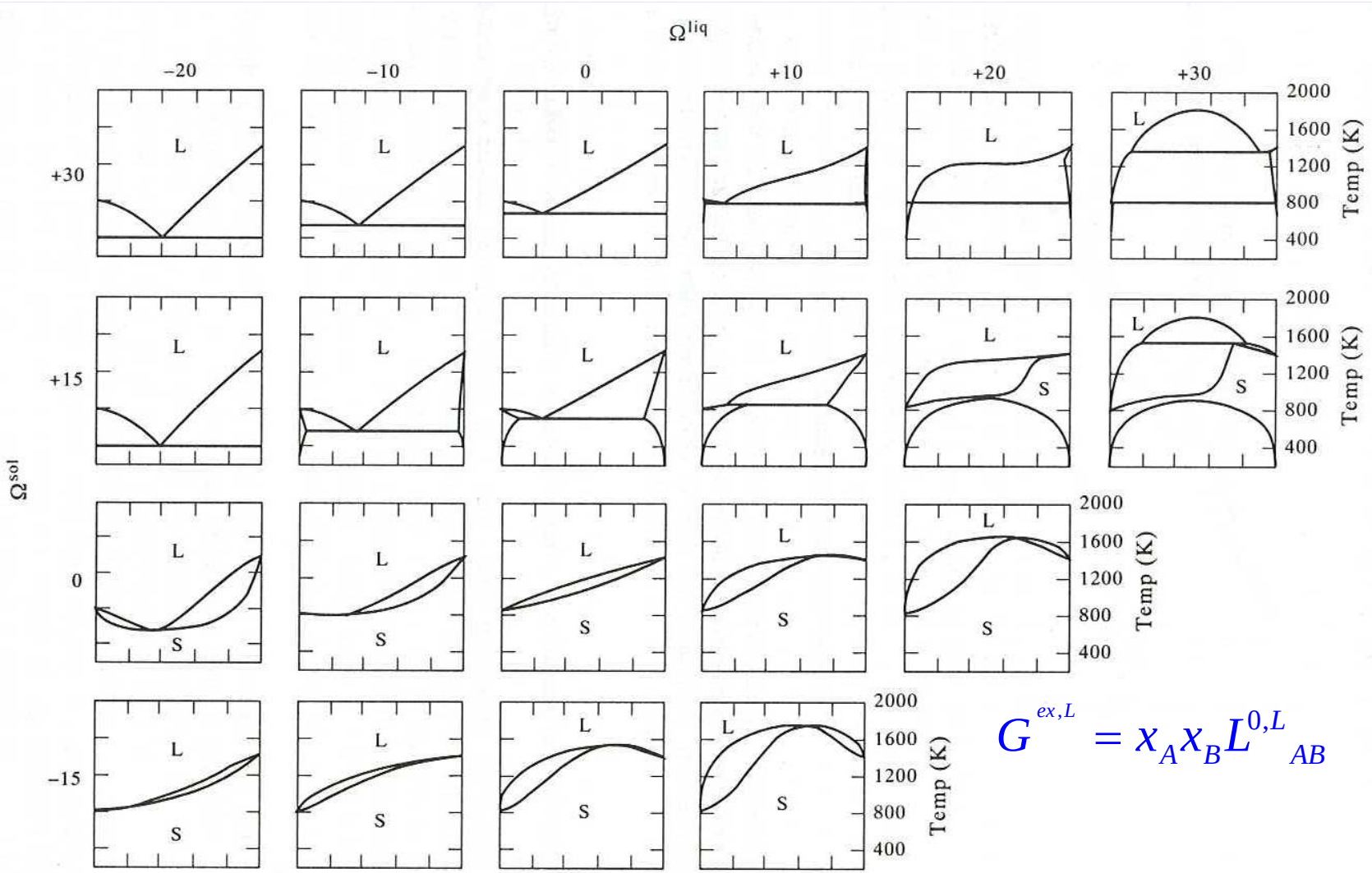

$$G^{ex,L} = x_A x_B L^{0,L}_{AB}$$

Figure 3.15. Topological features of phase diagrams calculated using regular solution theory.

Illustration Redlich-Kister contributions

$L^0_{AB} = L^1_{AB} = L^2_{AB} = L^3_{AB} = L^4_{AB} = -6000$

$T = cte$

$$G^{ex,\alpha} = x_A x_B L^{\nu}{}_{AB}(x_A - x_B)^{\nu}$$

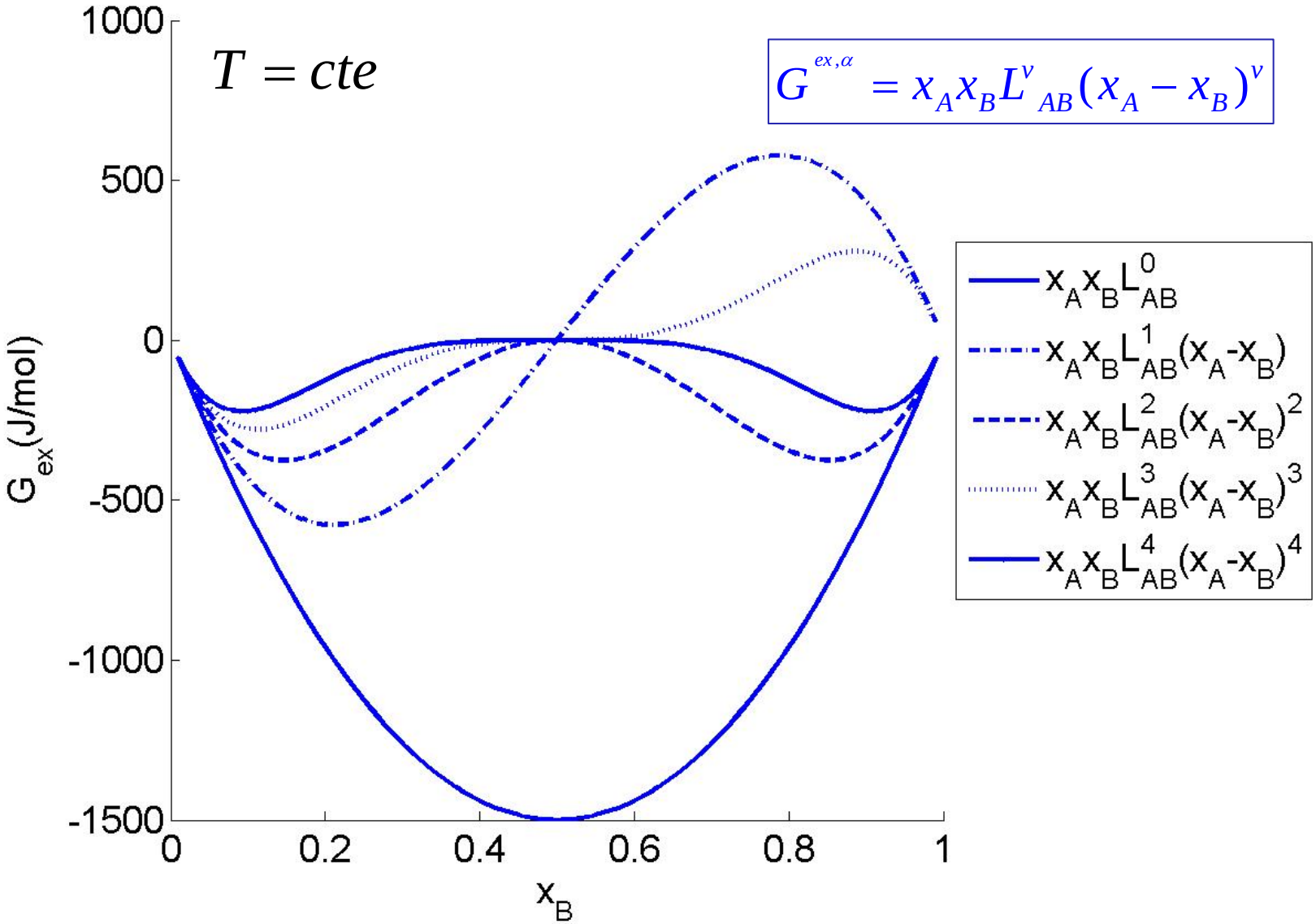

Illustration Redlich-Kister ...ns

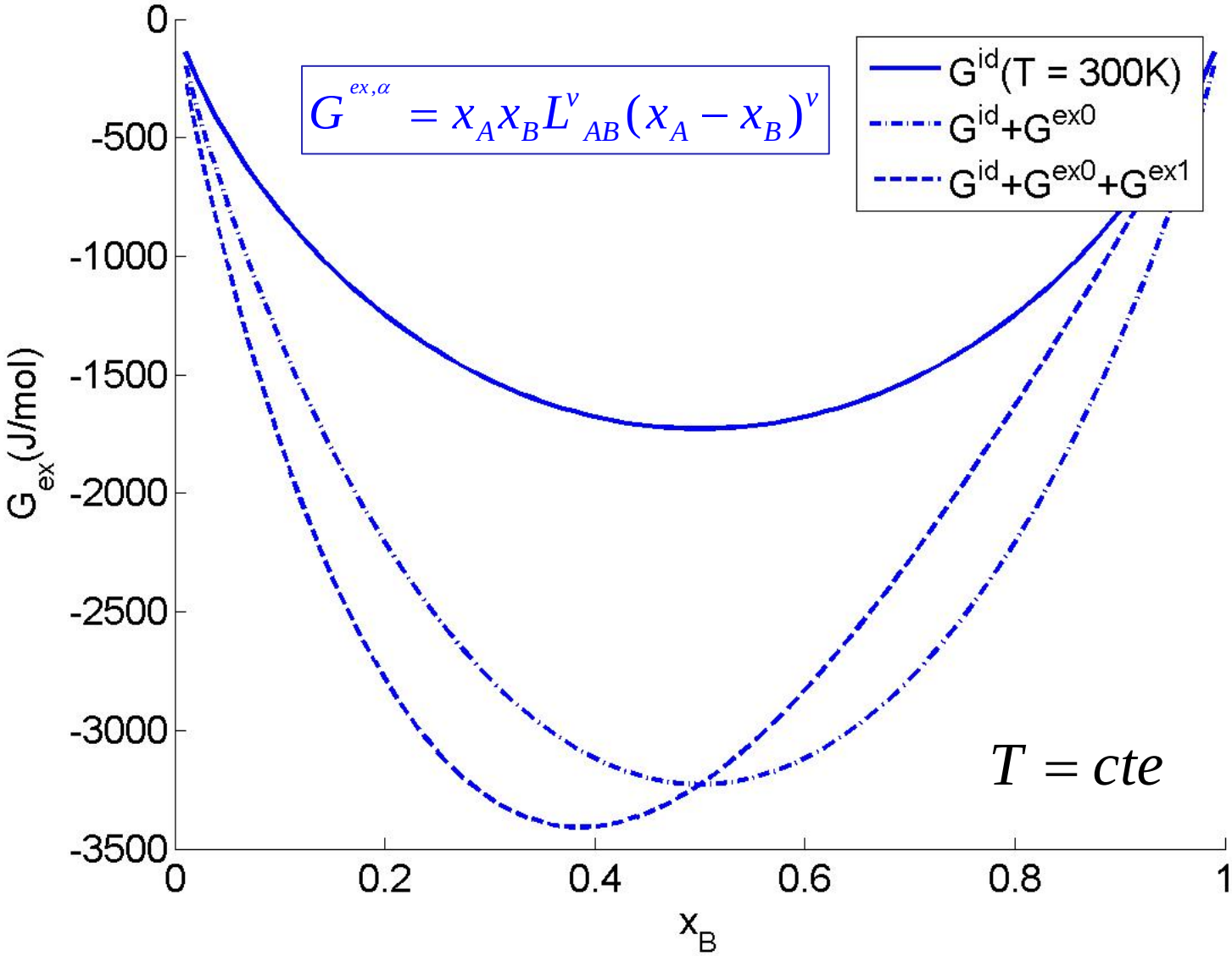

Extrapolation to higher-order systems

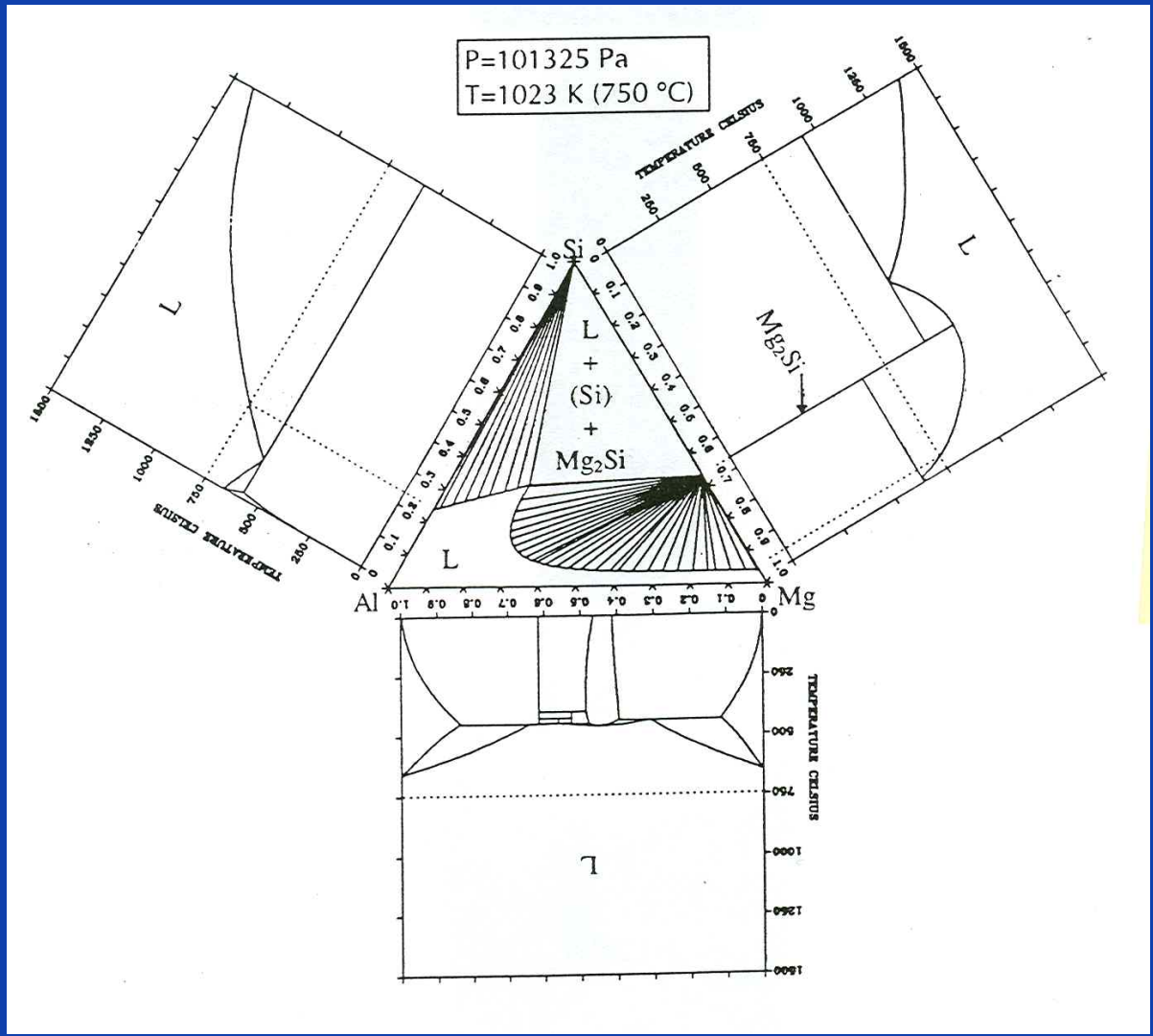

Extrapolation models

- **Extrapolation schemes**

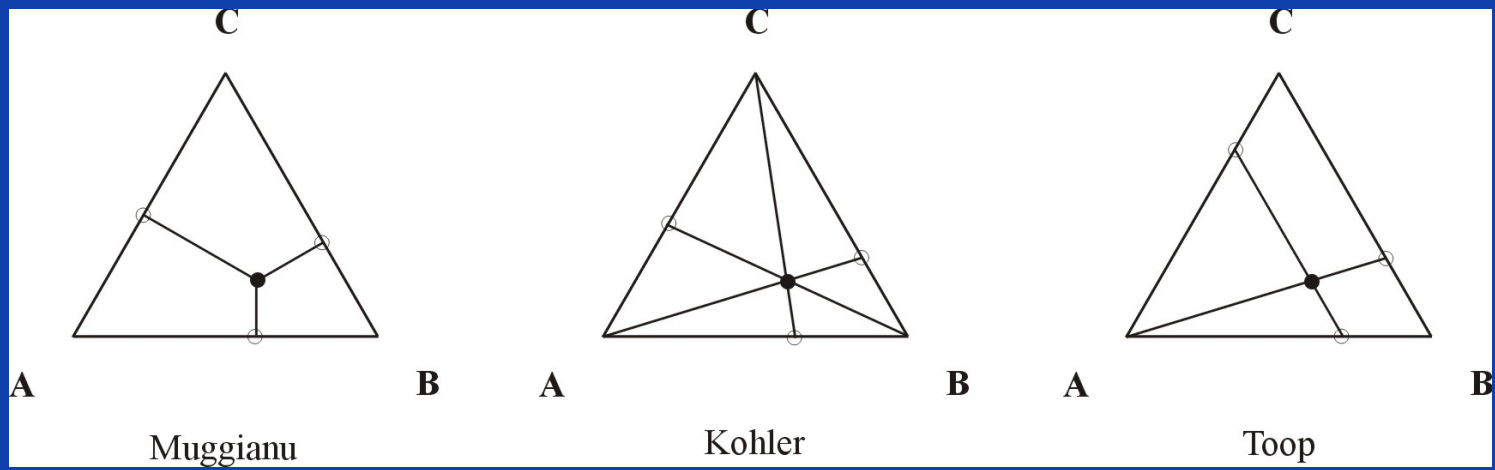

- **Redlich-Kister-Muggianu**

$$G^{ex} = G^{ex}_{AB} + G^{ex}_{AC} + G^{ex}_{BC} + x_A x_B x_C (x_A L^0_{ABC} + x_B L^1_{ABC} + x_C L^2_{ABC})$$

Ternary substitutional alloys

- **General expression** $G - G^{ref} = G^{id} + G^{ex} + G^{phys}$
  - **Mechanical mixing of pure elements**

$$G^{ref,\alpha} = x_A G_A^{0,\alpha} + x_B G_B^{0,\alpha} + x_C G_C^{0,\alpha}$$

  - **Ideal mixing (Raoults solution)**

$$G^{id} = x_A \ln(x_A) + x_B \ln(x_B) + x_C \ln(x_C)$$

  - **Excess interactions, Redlich-Kister-Muggianu**

$$G^{ex} = G_{AB}^{ex} + G_{AC}^{ex} + G_{BC}^{ex} + x_A x_B x_C (x_A L^0{}_{ABC} + x_B L^1{}_{ABC} + x_C L^2{}_{ABC})$$

    - **T-dependence** $L^{v}{}_{ABC} = a + bT$
    - **G^{ex}_{AB} from binary optimizations**
    - **$L_{ABC}{}^{v}$ from experiments**

Sublattice models

- **Phases with ordering**
  - **Mixing only allowed within certain sublattices, represented as $(A,B)_{a1}(A,Va)_{a2}$**

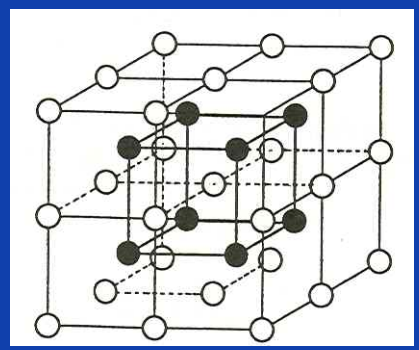

  - **Intermetallic compound, FeTi $\rightarrow$(%Fe,Ti)(Fe,%Ti), Fe_2Ti $\rightarrow$(%Fe,Ti)$_2$(Fe,%Ti), B_2Ti $\rightarrow(B)_2(Ti)$**
  - **Interstitial phases, $(Cr,Fe,Ni,\ldots)_{a1}(C,N,H,Va,\ldots)_{a2}$**

- **Molar fraction $\rightarrow$ *lattice fractions* ^1y_A, ^2y_A, ^1y_B, $^2y_{Va}$**

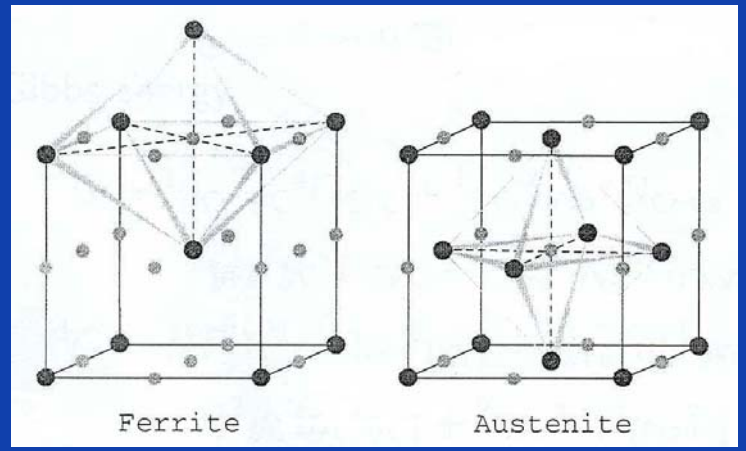

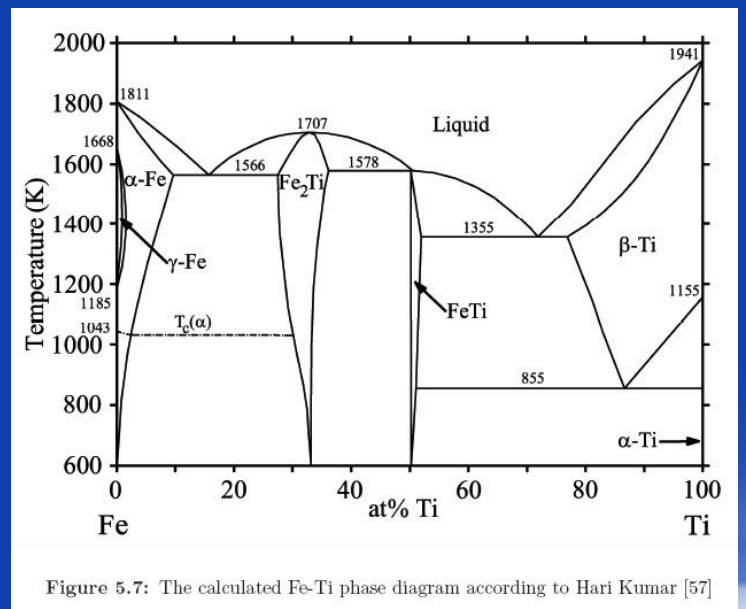

Figure 5.7: The calculated Fe-Ti phase diagram according to Hari Kumar [57]

KATHOLIEKE UNIVERSITEIT LEUVEN

thermo research group

Quantitative and thermodynamically consistent phase-field model for multi-phase systems

Multi-grain and multi-phase structures

- **Single phase-field models -> Multiple phase-field models**

$$\eta \rightarrow \{\eta_1, \eta_2, \eta_3, \ldots, \eta_p\}$$

$$(\eta_1, \eta_2, \ldots, \eta_i, \ldots, \eta_p) = (0, 0, \ldots, 1, \ldots, 0)$$

  - **Model extension**

$$F(\eta_1, \eta_2, \eta_3, \ldots, |\nabla \eta_1|^2, |\nabla \eta_2|^2, \ldots)$$

    - **Different types of interfaces**
    - **Triple and higher order junctions**

  - **Numerically**
    - **Same accuracy for all interfaces and phases**
    - **All interfaces within range of validity of the thin interface asymptotics**

$$\rightarrow \ell_{num} = cte$$

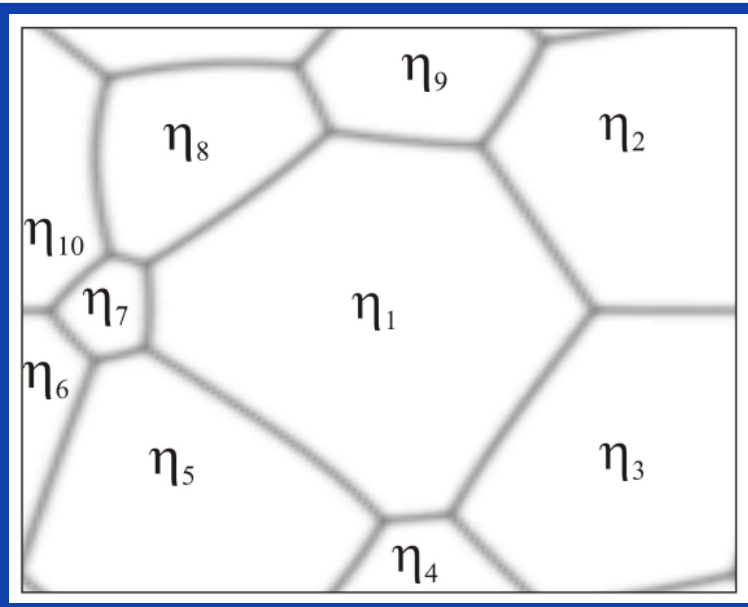

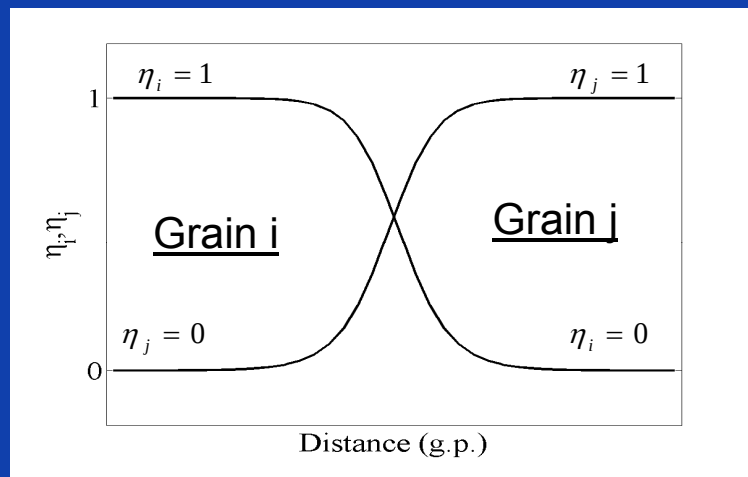

KATHOLIEKE UNIVERSITEIT LEUVEN

Multi-grain and multi-phase models: major difficulties

- **Third-phase contributions**
  - $\sigma_{12} = \sigma_{13} = 7/10\ \sigma_{12}$

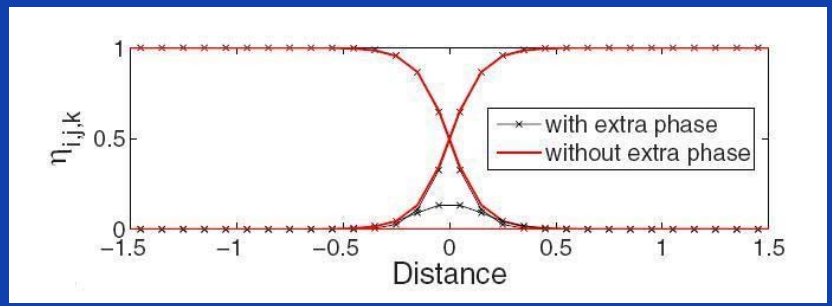

  - → **Careful choice of multi-well function and gradient contribution**

η_3

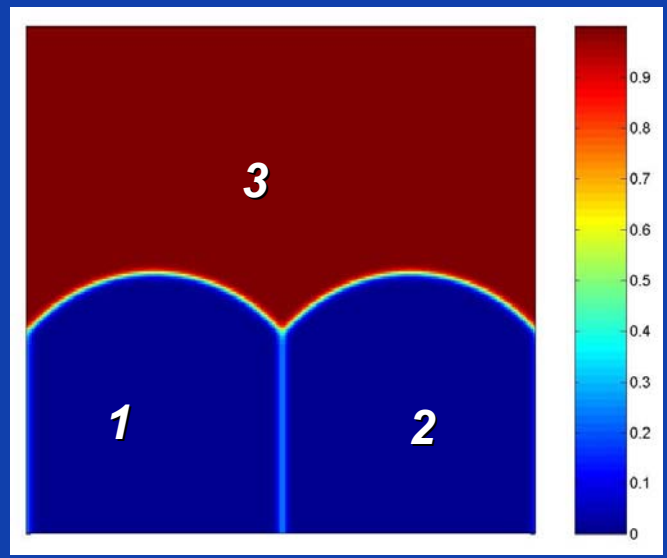

- **Interpolation function**
  - **Zero-slope at equilibrium values of the phase fields**
  - **Thermodynamic consistency**

$$f_{chem} = \sum_{i=1}^{p} h_i(\eta_1, \eta_2, \ldots) f^i(c,T) \quad \Rightarrow \sum_{i=1}^{p} h_i(\eta_1, \eta_2, \ldots) = 1$$

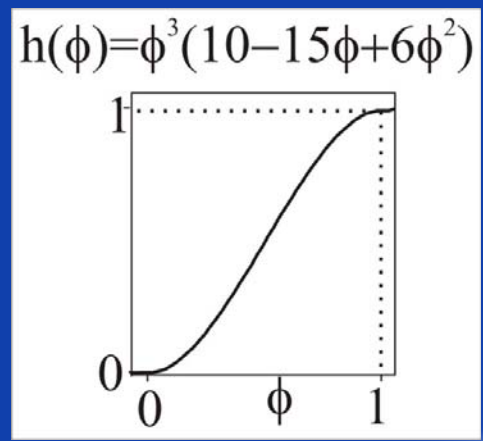

KATHOLIEKE UNIVERSITEIT LEUVEN

Extension to multi-component multi-phase alloys

- **Phase field variables:**
  - **Grains** $\eta_{\alpha 1}, \eta_{\alpha 2}, \ldots, \eta_{\alpha i}(\vec{r}, t), \ldots,$ $\eta_{\beta 1}, \eta_{\beta 2}, \ldots \eta_p$
  - **Composition** $c_A, c_B(\vec{r}, t), \ldots, c_{C-1}$

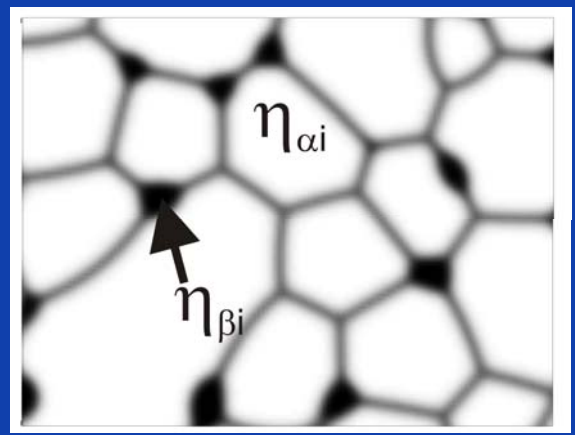

- **Bulk energy:** $f_{bulk}(c_k, \eta_{\rho i}) = \sum_{\rho} \phi_\rho f^\rho(c_k^\rho)$
  - **with**

$$\begin{cases} \dfrac{\partial f^\beta(c_k^\beta)}{\partial c_k^\beta} = \dfrac{\partial f^\alpha(c_k^\alpha)}{\partial c_k^\alpha} = \ldots = \tilde{\mu}_k \\ x_k = \sum_\rho \phi_\rho x_k^\rho \end{cases} \quad \textbf{and} \quad \phi_\rho = \frac{\sum_i \eta_{\rho i}^2}{\sum_{\pi=\alpha,\beta,\ldots} \sum_i \eta_{\pi i}^2}$$

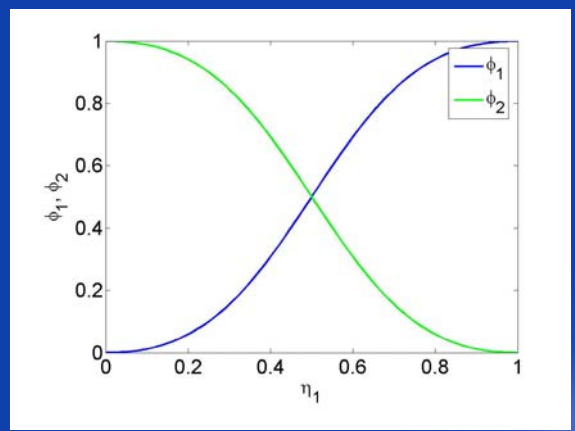

N. Moelans, Acta Mater. 2011.

KATHOLIEKE UNIVERSITEIT LEUVEN

Extension to multi-component multi-phase alloys

- **Bulk and interface diffusion:**

$$\frac{\partial x_k}{\partial t} = \nabla \cdot \left[\left(\sum_{\rho} \phi_\rho M_k^\rho + \sum_{\rho,i \neq \sigma,j} \eta_{\rho,i}^2 \eta_{\sigma,j}^2 \right) \nabla \mu_k \right]$$

With $M_k^\rho = \dfrac{D_k^\rho}{\dfrac{\partial^2 f_m^\rho}{\partial x_k^2}}$ **and** $M_{interf} = 3 \left(\dfrac{D_{interf}}{\partial^2 f^m / \partial x_k^2} \right) \left(\dfrac{\delta_{gb}}{\delta_{num}} \right)$

- **Interface movement:**

$$\frac{\partial \eta_{i\rho}}{\partial t} = -L \frac{\delta F(\eta_{i\rho}, x_k)}{\delta \eta_{i\rho}}$$

  - **Between phase α and β**

$$\frac{\partial \eta_{\alpha i}}{\partial t} = -L \left(g_{\text{int}}(\eta, \nabla \eta) + \frac{2 \eta_{\alpha i} \eta_{\beta j}^2}{\left(\eta_\alpha^2 + \eta_\beta^2 \right)^2} \left(f^\alpha(c^\alpha) - f^\beta(c^\beta) - (c^\alpha - c^\beta)\mu \right) \right)$$

Curvature driven *Bulk energy driven*

Numerical validation for multi-component multi-phase model

- Triple junction

- Growing sphere

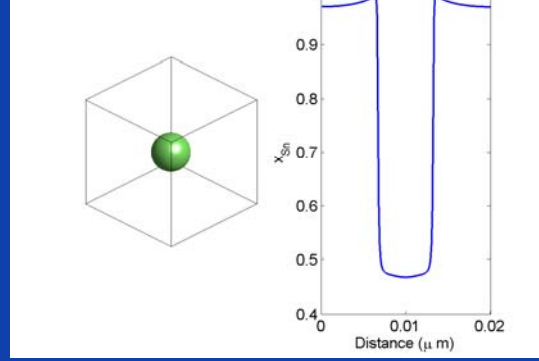

- Intermediate phase

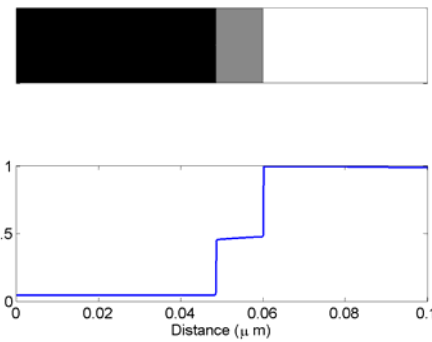

- Coarsening

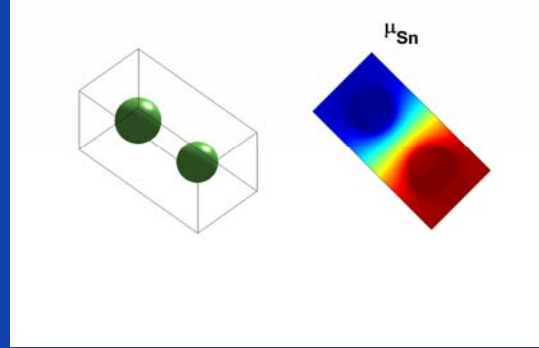

- Processes for which v(t) ↘
- Conclusions for grain growth model remain
  - Accuracy controlled by $\ell_{num} / \Delta x$
  - Diffuse interface effects for $\ell_{num} / R > 5$
  - Angles outside [100°-140°] require larger resolution $\ell_{num} / \Delta x$ for same accuracy

N. Moelans, Acta Mater. 2011.

KATHOLIEKE UNIVERSITEIT LEUVEN

thermo research group

Coupling phase-field with thermodynamics databases

Phase diagram

- Ternary Ag-Cu-Sn, T = 180 °C

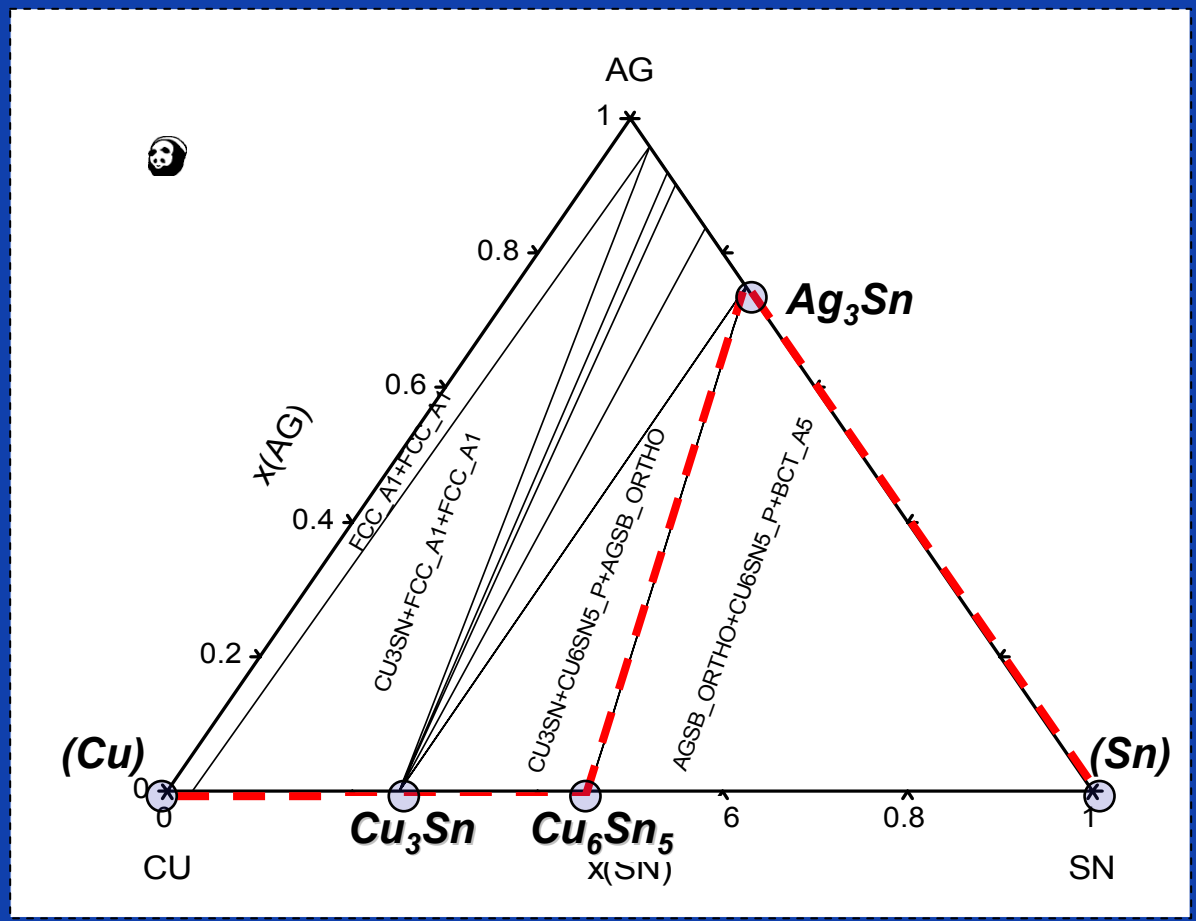

Phase diagram

- **Binary Cu-Sn**

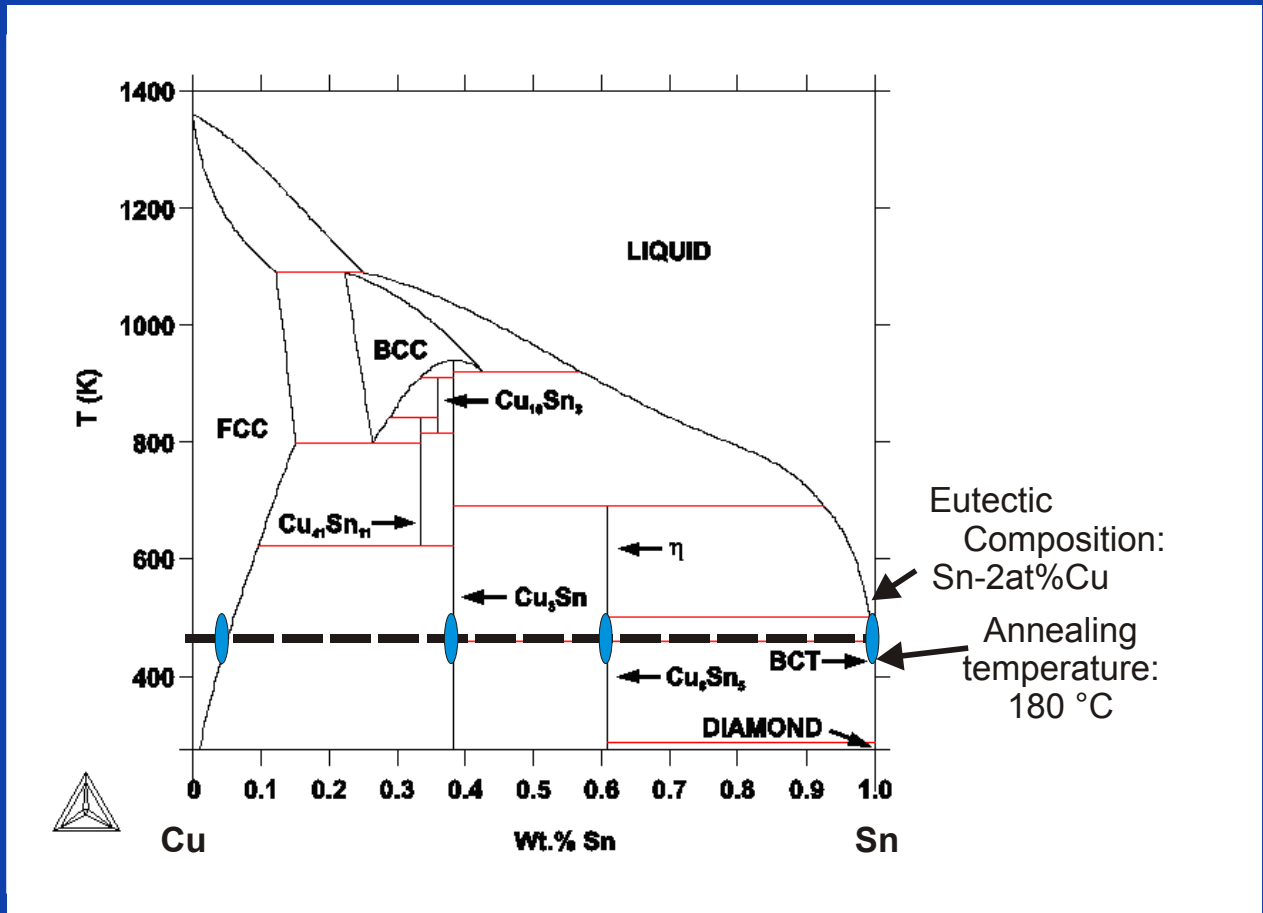

KATHOLIEKE UNIVERSITEIT LEUVEN

Parabolic composition dependence

- **Bulk energy** $f_{bulk}(\eta_i, x_{Sn}) = \sum_\rho \phi_\rho f^\rho(x_{Sn}^\rho) = \sum_\rho \phi_\rho \frac{G_m^\rho(x_{Sn}^\rho)}{V_m}$

- **Parabolic composition dependence**
  - **Simplifies solution phase-field equations**
  - **No composition dependence needed for D**

$$M^\rho = \frac{D^\rho}{\frac{\partial^2 f^\rho}{\partial x_{Sn}^2}} = \frac{D^\rho}{A^\rho}$$

  - **Difficult for higher order systems and large composition variations**

$$f^\rho = \frac{A^\rho}{2}\left(x_{Sn} - x_{Sn,0}\right)^2 + C^\rho$$

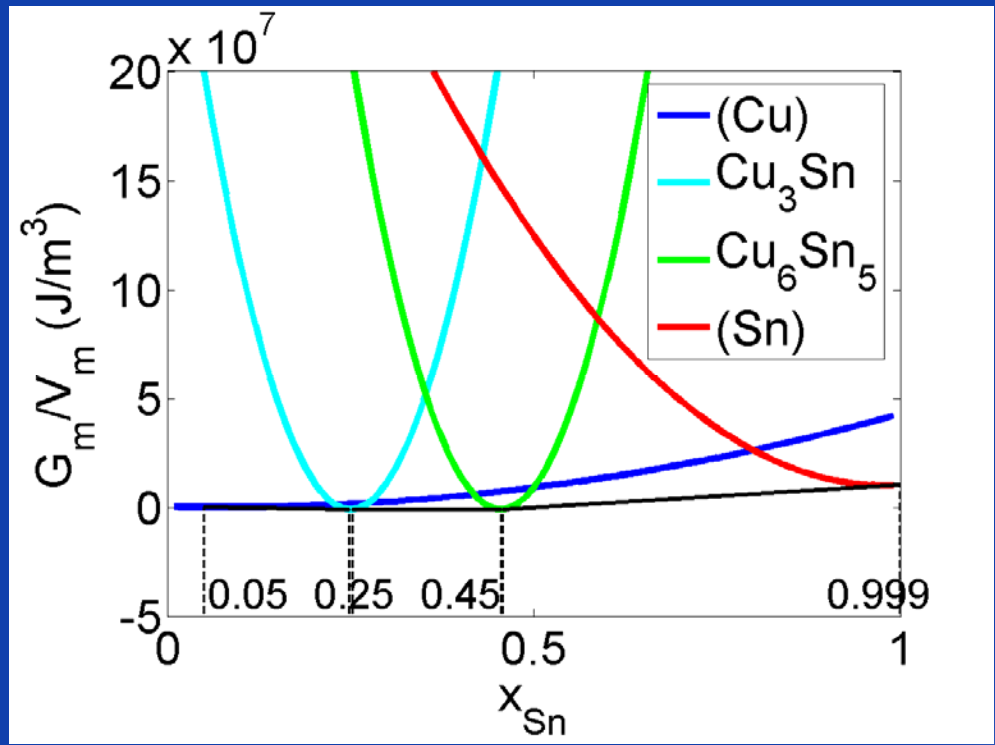

S.Y. Hu, J. Murray, H. Weiland, Z.-K. Liu, L.-Q. Chen, Comp. Coupl. Phase Diagr. Thermoch., 31 (2007) p 303

Coupling with thermodynamic database

- Free energies over full composition range are needed in phase-field
- Stoichiometric phases
  - Approximated as

$$G^{\rho} = \frac{A^{\rho}}{2}\left(x_{Sn} - x_{Sn,0}\right)^2 + C^{\rho}$$

$$C^{\rho} = G^{stoich}$$

$$x_{Sn,0} = x_{stoich}$$

  - Choice of A requires 'trial and error'
    - Numerics – Small shift in phase equilibria
    - Here: A = 1e6

Cu-Sn

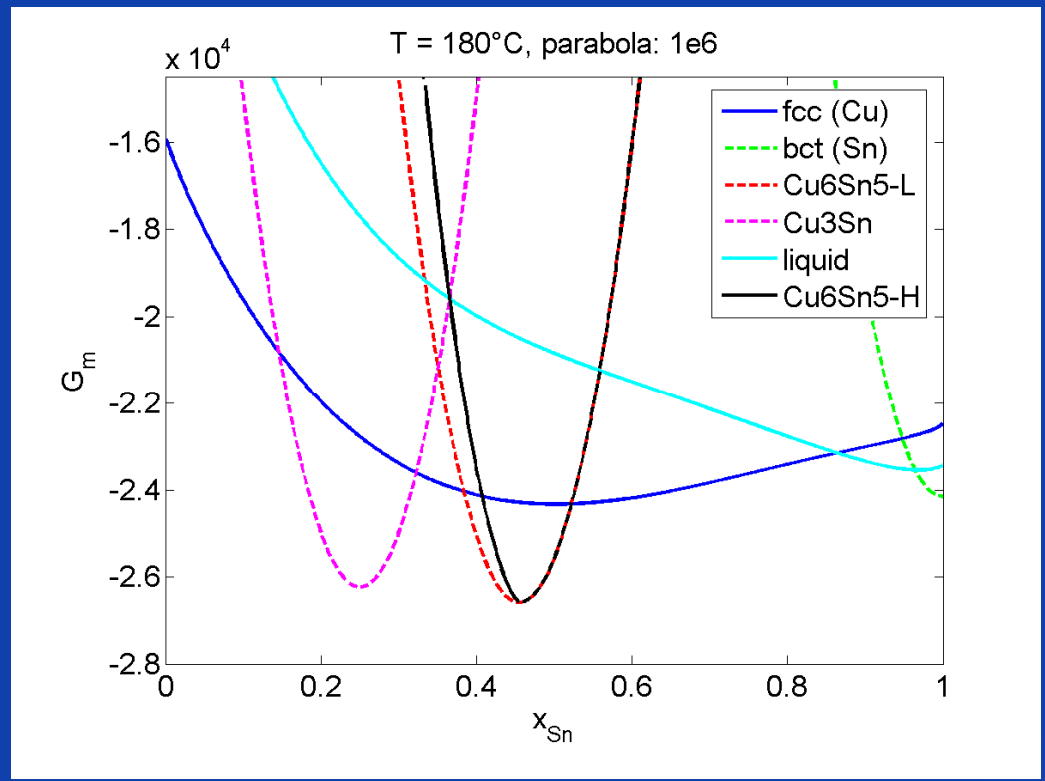

Gibbs energies from A. Dinsdale, A. Watson, A. Kroupa, J. Vřešťál, A. Zemanová, J. Vízdal COST 531-Lead Free Solders: Atlas of Phase Diagrams for Lead-Free Soldering, vols. 1,2 (2008) ESC-Cost office

Coupling with thermodynamic database

Ag-Cu-Sn

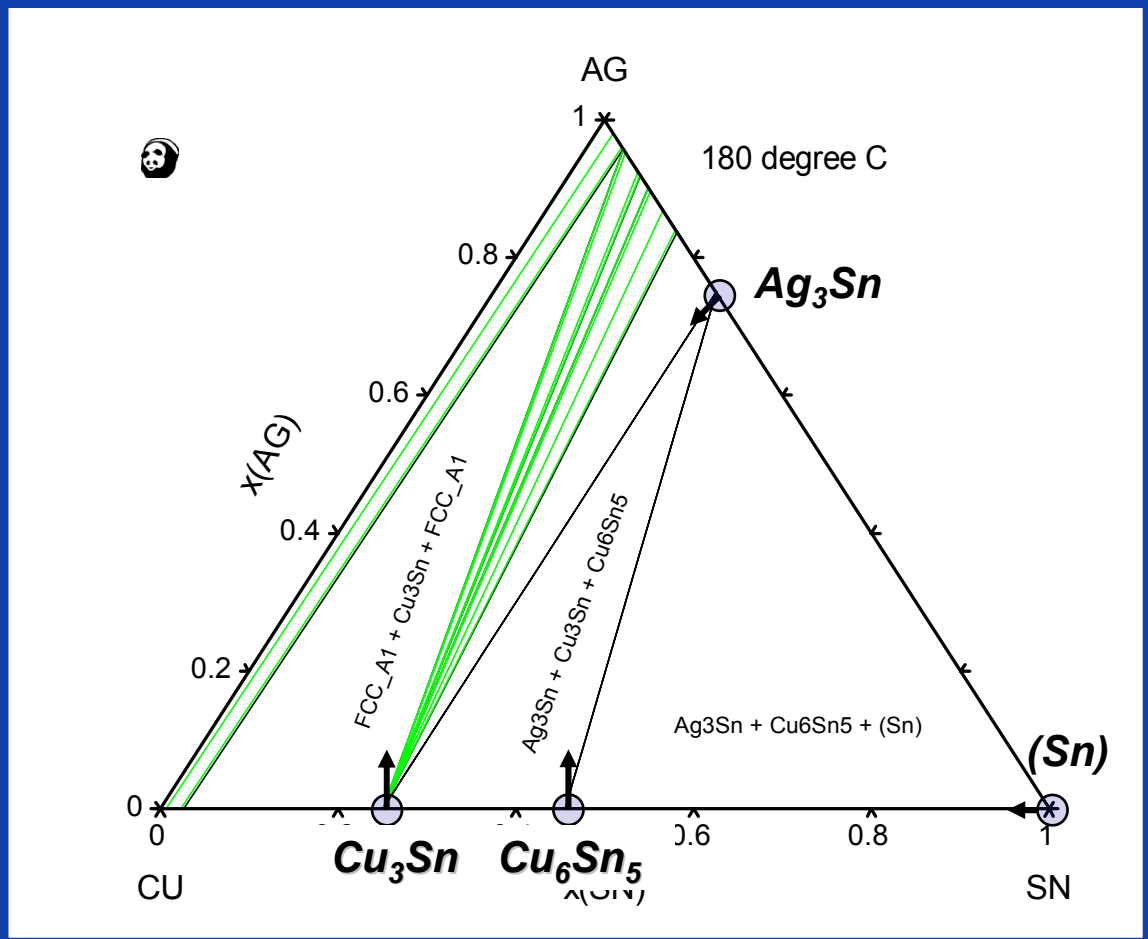

- **Binary phases shifted into ternary, e.g.**

$$G^{Ag3Sn} = G^{Ag3Sn}(x'_{Ag}, x'_{Sn}) + \frac{A}{2}(x_{Sh} - x_{Cu})^2$$

With

$$x'_{Ag} = (1 - x_{Sh})x_{Ag}$$
$$x'_{Sn} = (1 - x_{Sh})x_{Sn}$$

$$A = 1e6$$
$$x_{Sh} = 0.001$$

KATHOLIEKE UNIVERSITEIT LEUVEN

Coupling with thermodynamic database

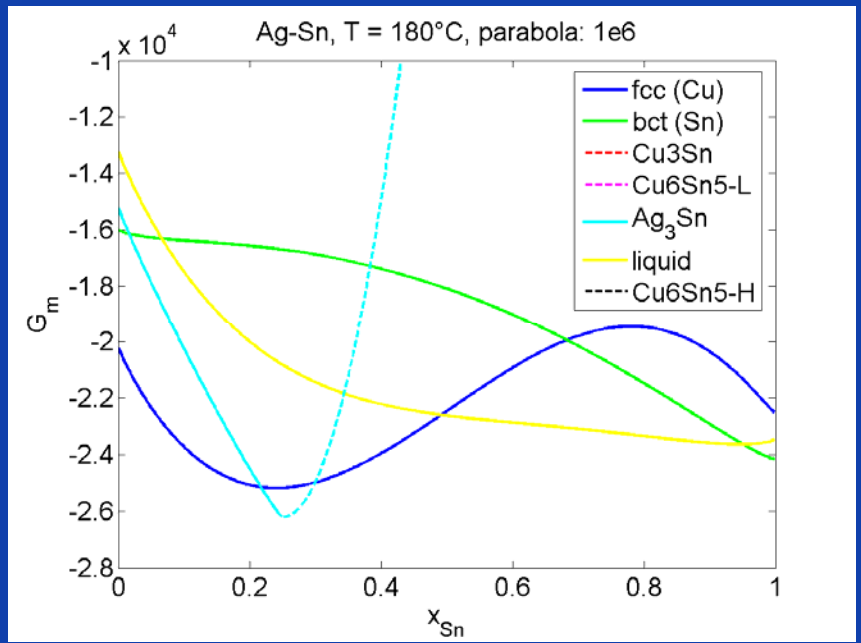

Ag-Sn-0.001Cu

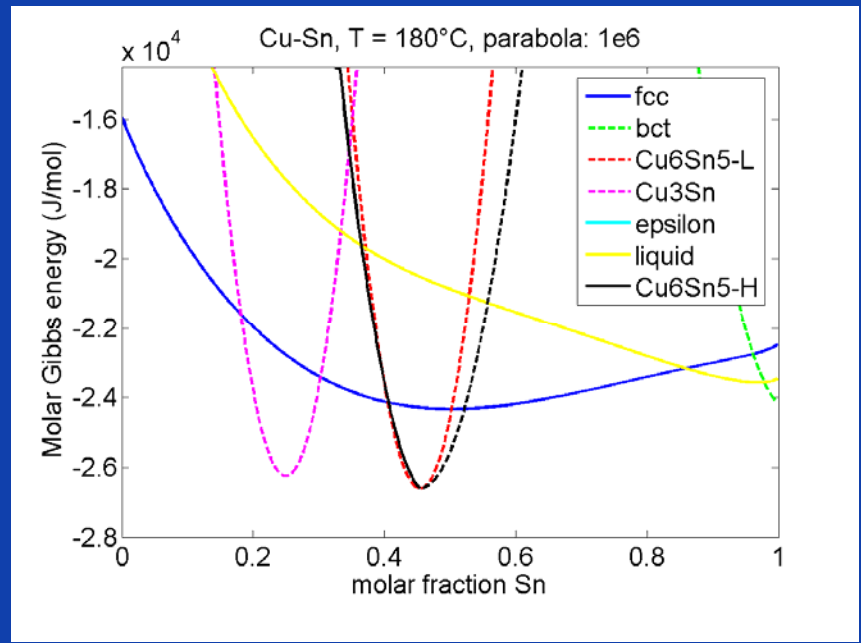

Cu-Sn-0.001Ag

- ***Sublattice model + parabolic extension***
  - ***Cu_6Sn_5-H: $(Cu)_{.545}:(Cu,Sn)_{.122}:(Sn)_{.333}$***
  - ***Ag_3Sn: $(Ag)_{.75}(Ag,Sn)_{.25}$***

Coupling with thermodynamic database

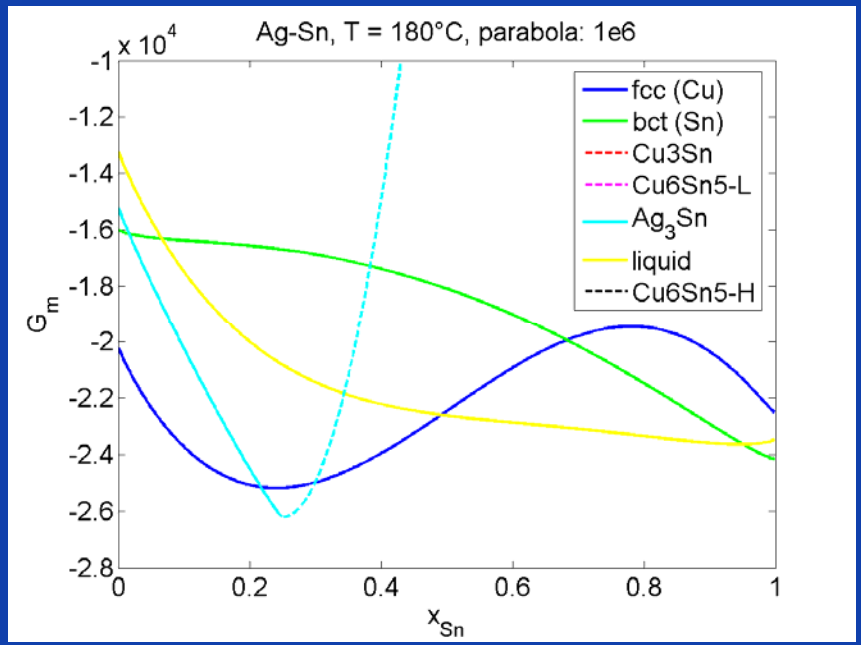

Ag-Sn-0.001Cu

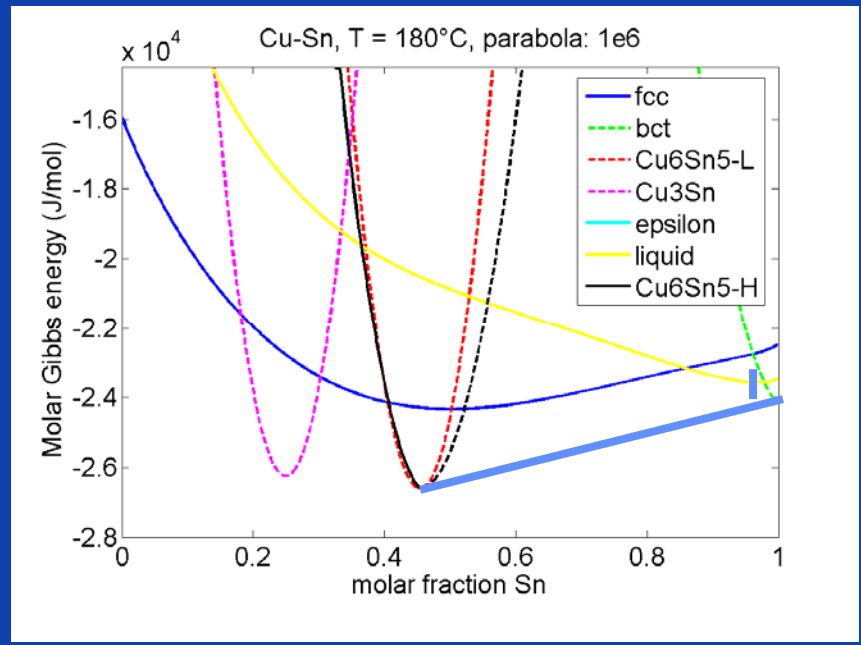

Cu-Sn-0.001Ag

- ***Sublattice model + parabolic extension***
  - ***Cu_6Sn_5-H: $(Cu)_{.545}:(Cu,Sn)_{.122}:(Sn)_{.333}$***
  - ***Ag_3Sn: $(Ag)_{.75}(Ag,Sn)_{.25}$***

KATHOLIEKE UNIVERSITEIT LEUVEN

Coupling with thermodynamic database

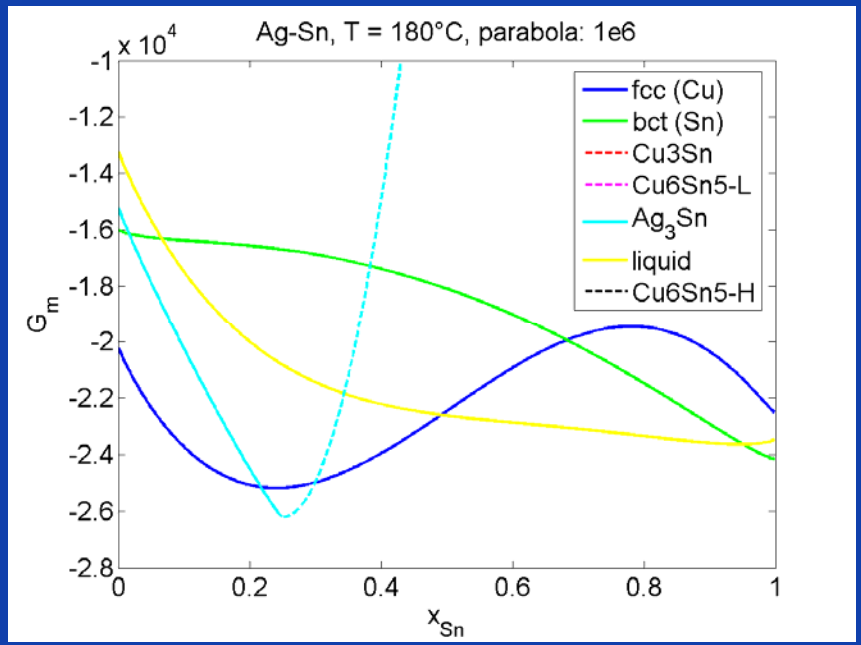

Ag-Sn-0.001Cu

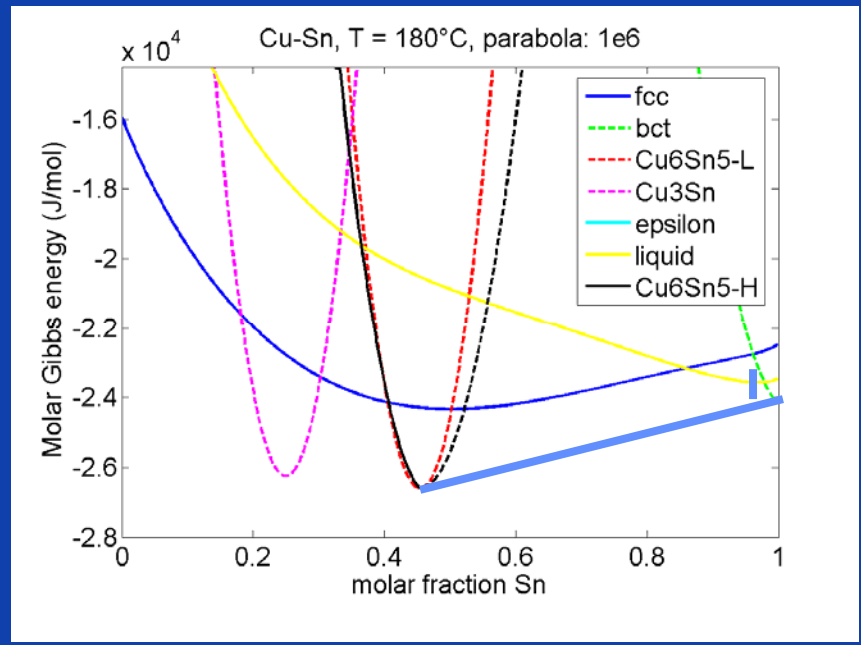

Cu-Sn-0.001Ag

- **Sublattice model + parabolic extension**
  - Cu_6Sn_5-H: $(Cu)_{.545}:(Cu,Sn)_{.122}:(Sn)_{.333}$
  - Ag_3Sn: $(Ag)_{.75}(Ag,Sn)_{.25}$

→ $G^{\rho}(x_{Ag},x_{Cu},x_{Sn})$ over full composition range

KATHOLIEKE UNIVERSITEIT LEUVEN

thermo research group

Interdiffusion and intermetallic growth in Cu/Sn-Cu solder joints

System properties

- **Equilibrium compositions**

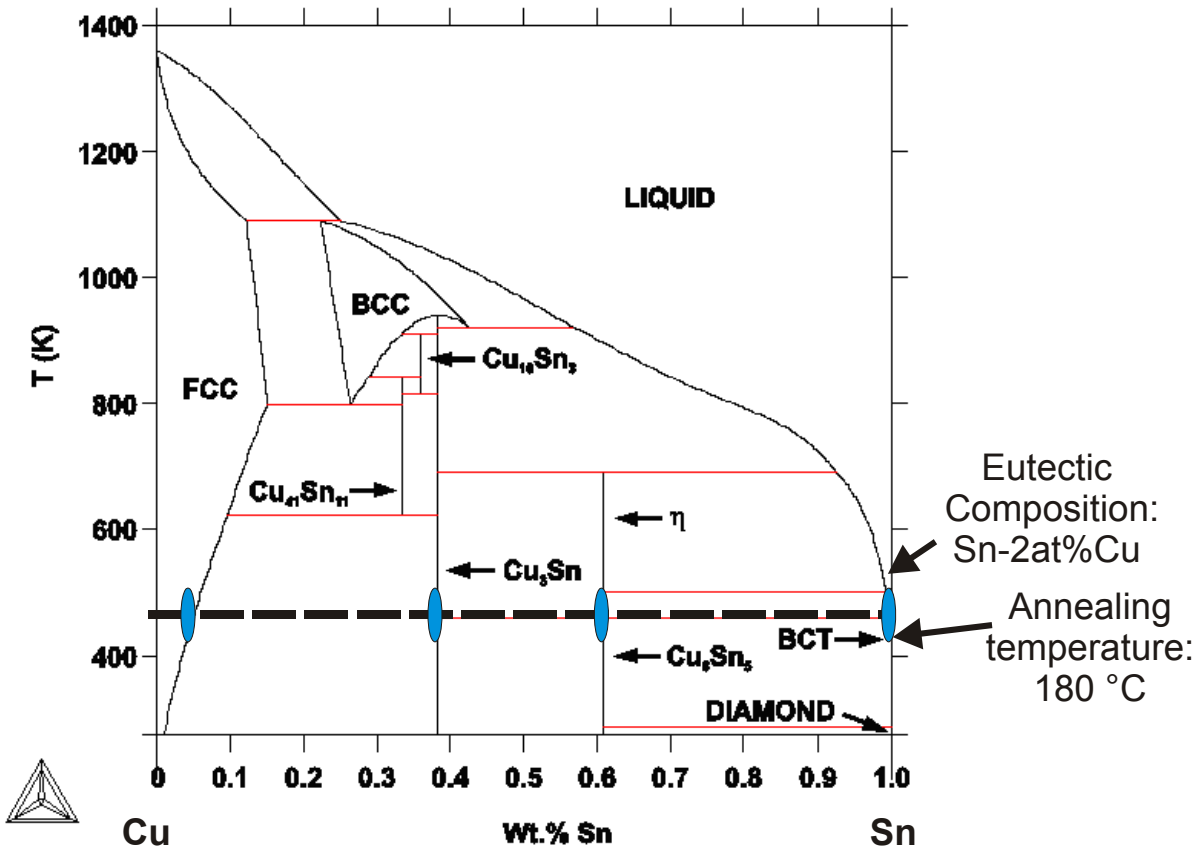

- **Interdiffusion coeffcients**

$$D_{Sn}^{(Cu)} = 10^{-25}$$

$$D_{Sn}^{Cu3Sn} = 5 \cdot 10^{-16}\ \mathrm{m^2/s}$$

$$D_{Sn}^{Cu6Sn5} = 10^{-15}\ \mathrm{m^2/s}$$

$$D_{Sn}^{(Sn)} = 10^{-12}\ \mathrm{m^2/s}$$

- **Interfacial energy**

$$\gamma_{gb} = 0.25 \quad \mathrm{J/m^2}$$

IMC-layer growth (1D)

- **Effect of bulk diffusion coefficients**

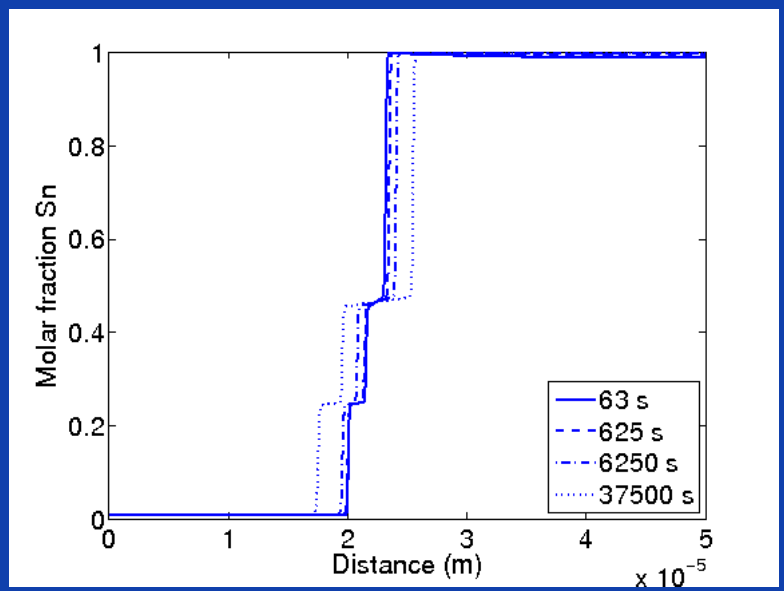

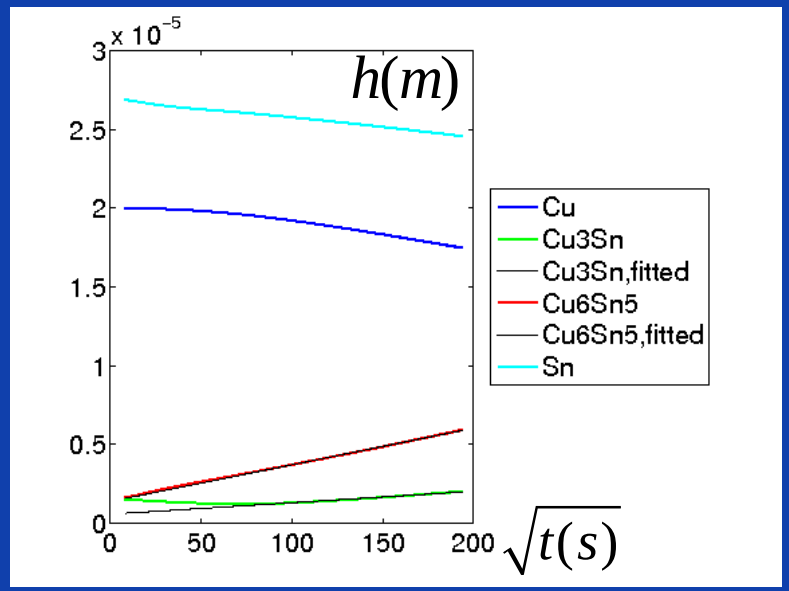

Diffusion coeffcients

$D_{Sn}^{(Cu)} = 10^{-25}\,\mathrm{m}^2/\mathrm{s}$

$D_{Sn}^{Cu3Sn} = 10^{-14}\,\mathrm{m}^2/\mathrm{s}$

$D_{Sn}^{Cu6Sn5} = 10^{-14}\,\mathrm{m}^2/\mathrm{s}$

$D_{Sn}^{(Sn)} = 10^{-12}\,\mathrm{m}^2/\mathrm{s}$

Initial composition

$x_{Sn,0}^{(Cu)} = 0.01 (< x_{Sn,eq}^{(Cu)})$

$x_{Sn,0}^{Cu3Sn} = 0.25$

$x_{Sn,0}^{Cu6Sn5} = 0.455$

$x_{Sn,0}^{(Sn)} = 0.99 (< x_{Sn,eq}^{(Sn)})$

$$\Rightarrow \quad k_{Cu3Sn} = 0.0073 \cdot 10^{-6}$$

$$k_{Cu6Sn5} = 0.023 \cdot 10^{-6}$$

KATHOLIEKE UNIVERSITEIT LEUVEN

IMC-layer growth (1D)

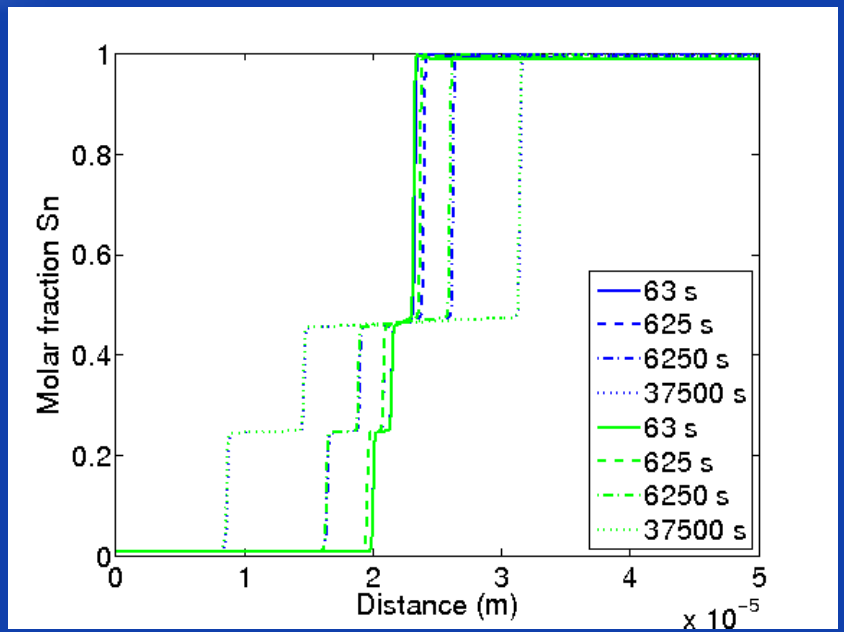

$D_{Sn}^{(Sn)} = 10^{-12}\,\mathrm{m}^2/\mathrm{s}$

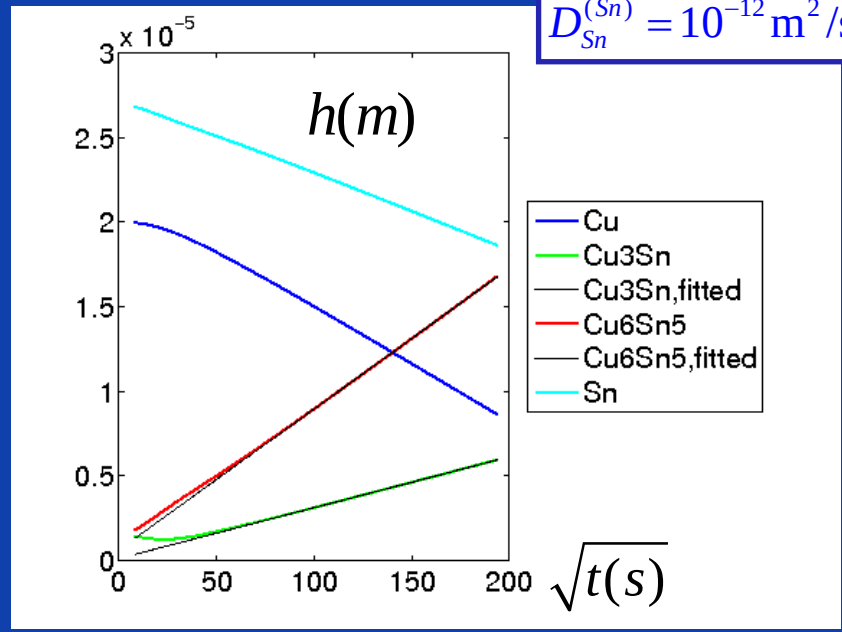

$$D_{Sn}^{(Cu)} = 10^{-25}\,\mathrm{m}^2/\mathrm{s}$$
$$D_{Sn}^{Cu3Sn} = 10^{-13}\,\mathrm{m}^2/s$$
$$D_{Sn}^{Cu6Sn5} = 10^{-13}\,\mathrm{m}^2/\mathrm{s}$$
$$D_{Sn}^{(Sn)} = 10^{-12}\,\mathrm{m}^2/\mathrm{s}$$

$$D_{Sn}^{(Cu)} = 10^{-25}\,\mathrm{m}^2/\mathrm{s}$$
$$D_{Sn}^{Cu3Sn} = 10^{-13}\,\mathrm{m}^2/s$$
$$D_{Sn}^{Cu6Sn5} = 10^{-13}\,\mathrm{m}^2/\mathrm{s}$$
$$D_{Sn}^{(Sn)} = 10^{-14}\,\mathrm{m}^2/\mathrm{s}$$

$$\Rightarrow \quad k_{Cu3Sn} = 0.0301 \cdot 10^{-6}$$
$$k_{Cu6Sn5} = 0.0833 \cdot 10^{-6}$$

$$\Rightarrow \quad k_{Cu3Sn} = 0.0306 \cdot 10^{-6}$$
$$k_{Cu6Sn5} = 0.0849 \cdot 10^{-6}$$

Comparison with experimental data

Cu_3Sn, T = 180 °C

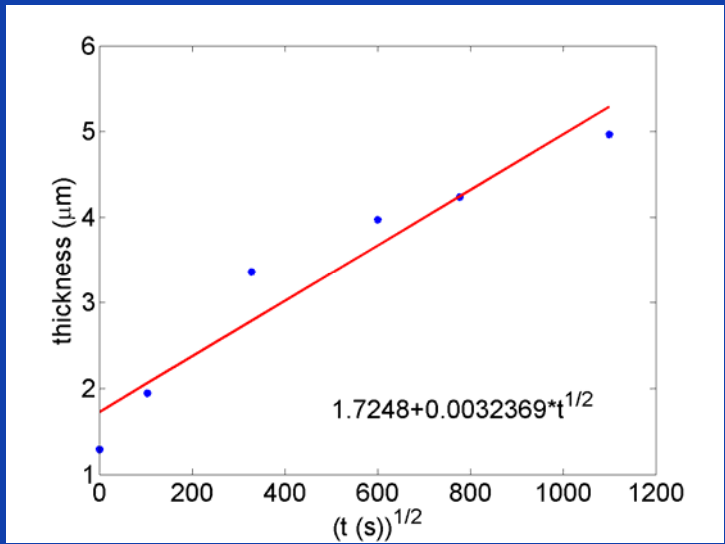

Cu_6Sn_5, T = 180 °C

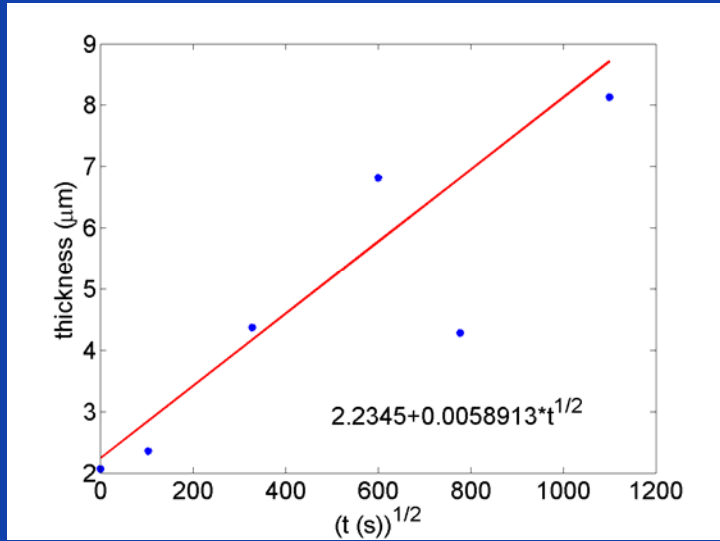

Parabolic growth constant experiments

T	k_Cu_3Sn	k_Cu_6Sn_5
150 °C	0.0010 10^{-6}	0.00032 10^{-6}
180 °C	0.0032 10^{-6}	0.0059 10^{-6}
200 °C	0.0043 10^{-6}	0.0071 10^{-6}

Parabolic growth constant in simulations with

$$D_{Sn}^{(Cu)} = 10^{-25}\,\mathrm{m}^2/\mathrm{s} \quad \Rightarrow \quad k_{Cu3Sn} = 0.0023 \cdot 10^{-6}$$

$$D_{Sn}^{Cu3Sn} = 10^{-15}\,\mathrm{m}^2/\mathrm{s} \qquad k_{Cu6Sn5} = 0.0073 \cdot 10^{-6}$$

$$D_{Sn}^{Cu6Sn5} = 10^{-15}\,\mathrm{m}^2/\mathrm{s}$$

$$D_{Sn}^{(Sn)} = 10^{-12}\,\mathrm{m}^2/\mathrm{s}$$

Data from J. Janckzak, EMPA

Effect of grain boundary diffusion

- **2D simulations**

$$D_{Sn}^{(Cu)} = 10^{-25}\,\mathrm{m}^2/\mathrm{s}$$
$$D_{Sn}^{Cu3Sn} = 10^{-15}\,\mathrm{m}^2/\mathrm{s}$$
$$D_{Sn}^{Cu6Sn5} = 10^{-15}\,\mathrm{m}^2/\mathrm{s}$$
$$D_{Sn}^{(Sn)} = 10^{-12}\,\mathrm{m}^2/\mathrm{s}$$
$$\mathrm{D}_{Sn}^{surf} = 0.66\cdot 10^{-9}\,\mathrm{m}^2/\mathrm{s}$$
$$\delta_{gb} = 1nm$$

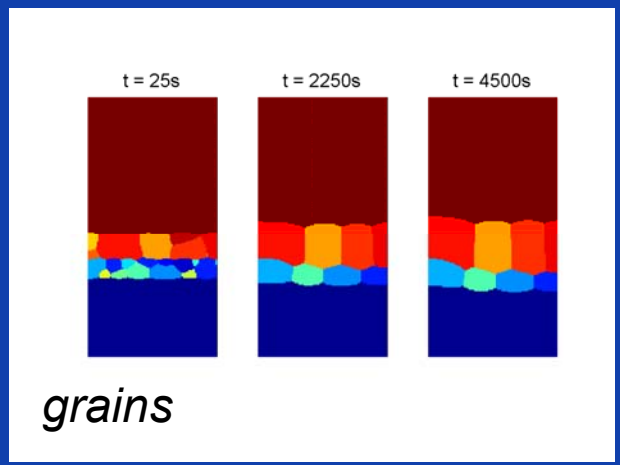

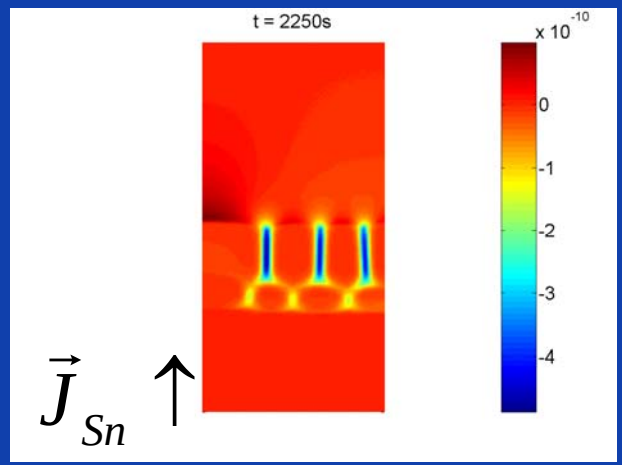

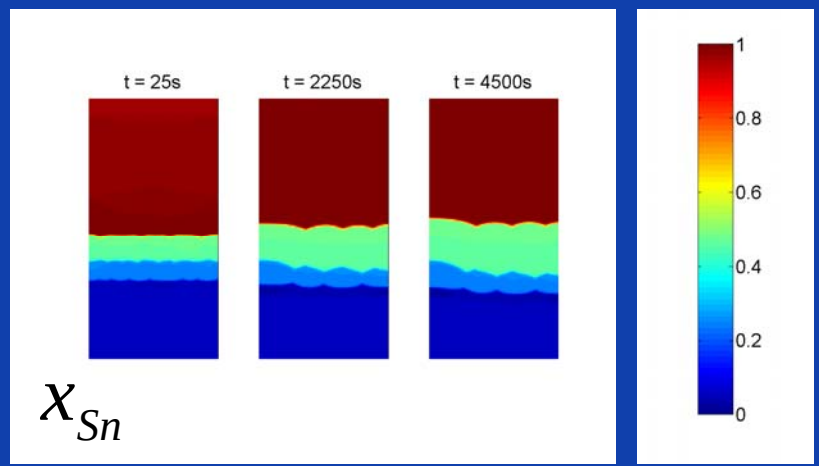

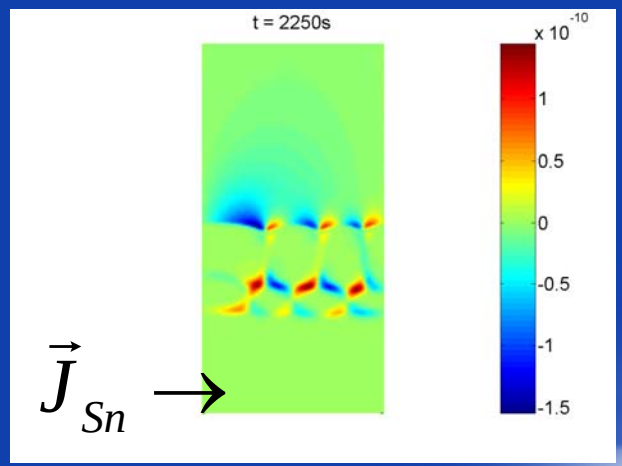

Effect of grain boundary diffusion

- **3D simulations**

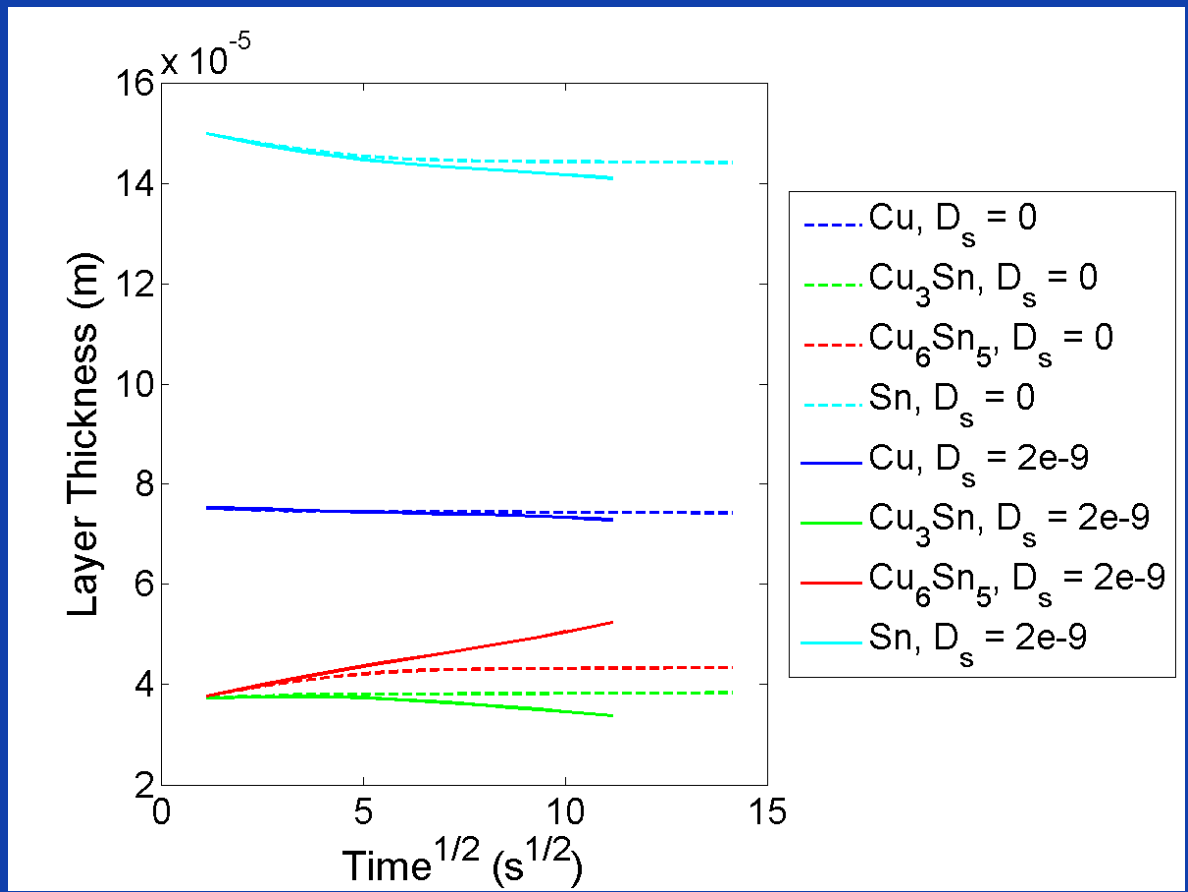

$D_{Sn}^{(Cu)} = 2 \cdot 10^{-25} \mathrm{m}^2/\mathrm{s}$

$D_{Sn}^{Cu3Sn} = 2 \cdot 10^{-15} \mathrm{m}^2/\mathrm{s}$

$D_{Sn}^{Cu6Sn5} = 2 \cdot 10^{-15} \mathrm{m}^2/\mathrm{s}$

$D_{Sn}^{(Sn)} = 2 \cdot 10^{-12} \mathrm{m}^2/\mathrm{s}$

$\mathrm{D}_{interf} = 2 \cdot 10^{-9} \mathrm{m}^2/\mathrm{s} \quad \delta_{gb} = 1nm$

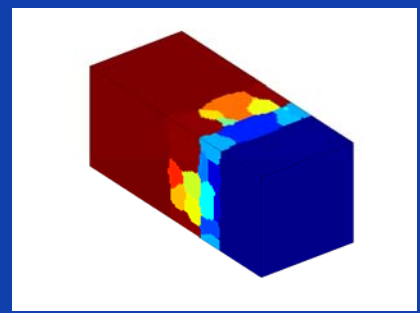

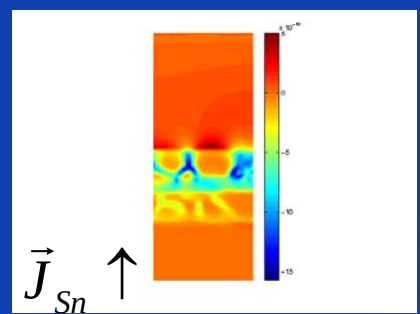

Growth behavior Cu_3Sn ?

Grain structure **Composition: x_{Sn}**

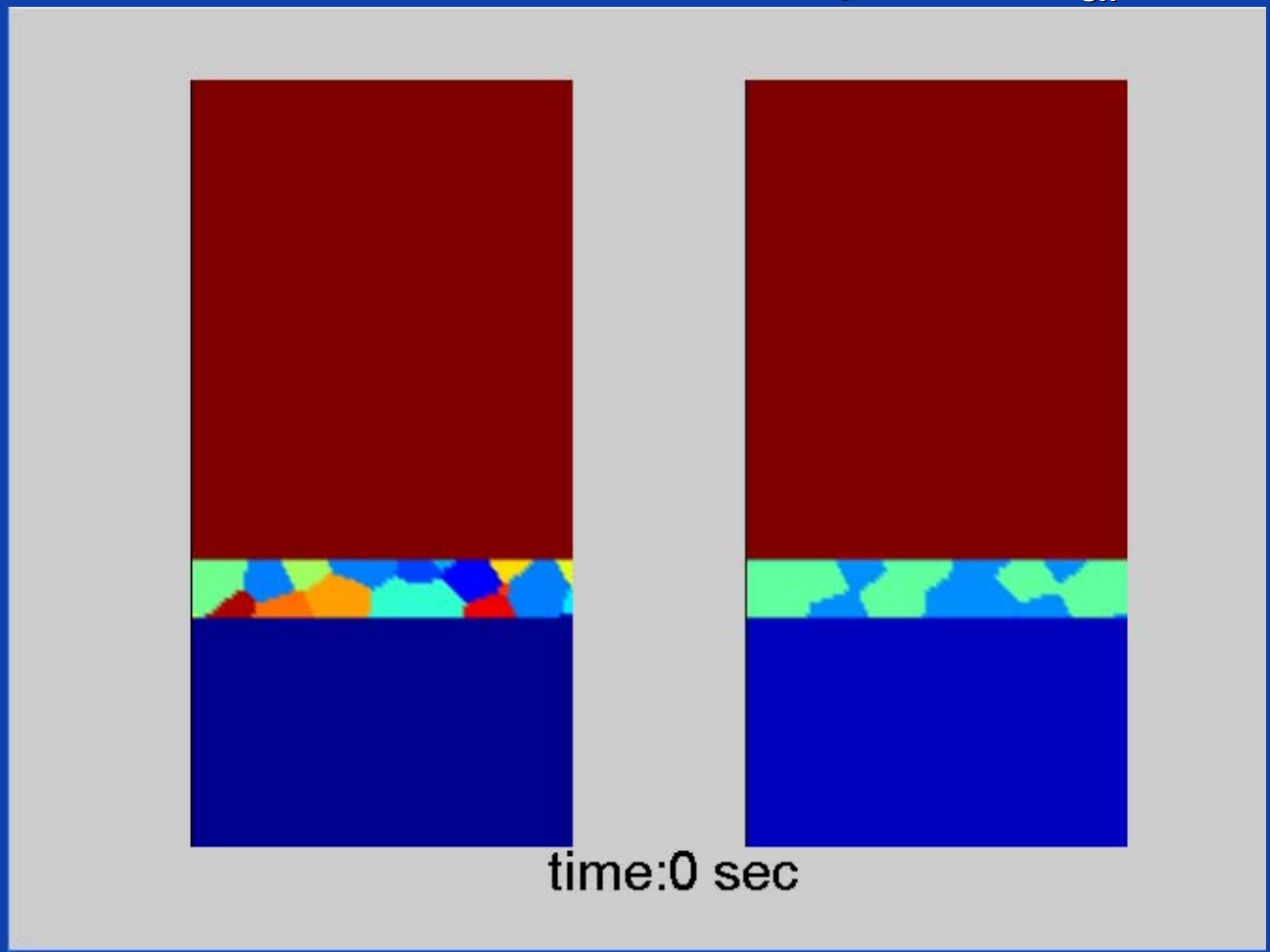

$$D_{Sn}^{(Cu)} = 2 \cdot 10^{-25}\,\mathrm{m}^2/\mathrm{s}$$

$$D_{Sn}^{Cu3Sn} = 2 \cdot 10^{-15}\,\mathrm{m}^2/\mathrm{s}$$

$$D_{Sn}^{Cu6Sn5} = 2 \cdot 10^{-15}\,\mathrm{m}^2/\mathrm{s}$$

$$D_{Sn}^{(Sn)} = 2 \cdot 10^{-12}\,\mathrm{m}^2/\mathrm{s}$$

$$\mathrm{D}_{Sn}^{surf} = 2 \cdot 10^{-12}\,\mathrm{m}^2/\mathrm{s}$$

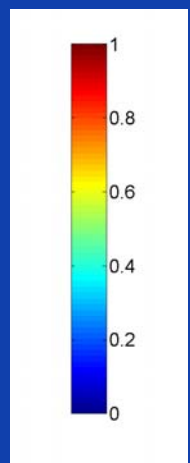

IMC growth in Sn-2at%Cu

- ***Initial compositions***

Solder:
$x_{Sn,0} = 0.98$

(Sn)-matrix
$x_{Sn} = 0.999$

Cu_6Sn_5-precipitates
$x_{Sn} = 0.4545$

IMC layer
Cu_6Sn_5
$x_{Sn} = 0.4545$

(Cu)-substrate
$x_{Sn} = 0.001$

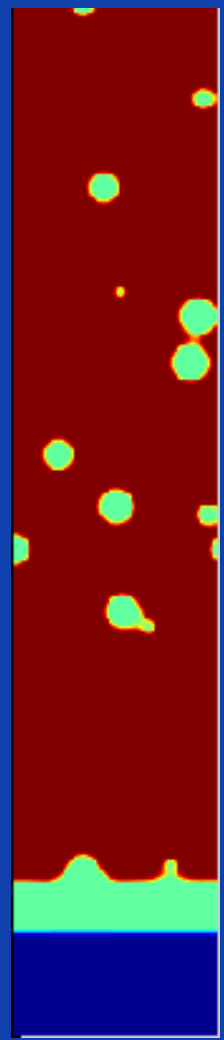

$$D_{Sn}^{(Cu)} = 10^{-25}\,\mathrm{m}^2/\mathrm{s}$$
$$D_{Sn}^{Cu6Sn5} = 10^{-16}\,\mathrm{m}^2/\mathrm{s}$$
$$D_{Sn}^{(Sn)} = 10^{-12}\,\mathrm{m}^2/\mathrm{s}$$

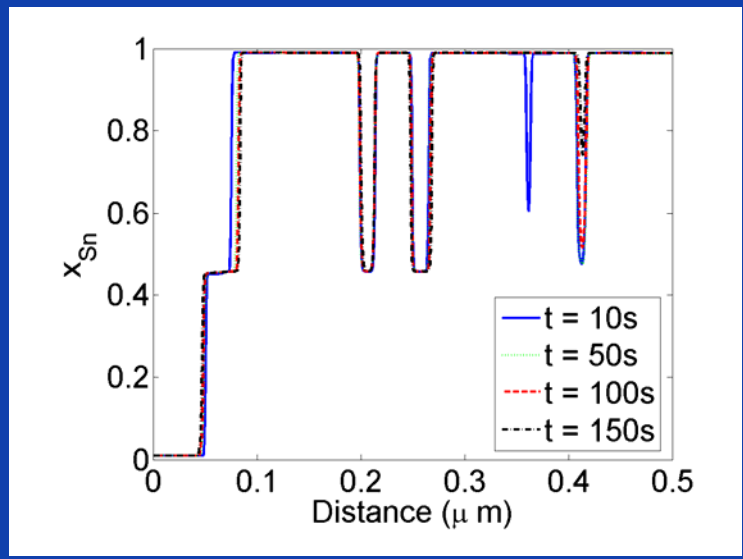

- **System size: 0.1μmx0.5μm**
- **Initially $f_V = 0.04$**
- **For future work: compare with experiments for nanoparticle-reinforced solders for which the grain size is known (J. Janczak, EMPA)**

KATHOLIEKE UNIVERSITEIT LEUVEN

Conclusions

- The phase-field implementation is able to reproduce thermodynamic and kinetic properties accurately
- Important to have realistic free energy functions and atomic diffusion mobilities for microstructure simulations
  - But how to treat stoichiometric phases, binary phases ?
  - Most general solution: Gibbs free energy over full composition range
- Powerful tool for the study of interdiffusion in joint materials

KATHOLIEKE UNIVERSITEIT LEUVEN

Thank you for your attention ! Questions ?

- **Acknowledgements**
  - **Research Foundation - Flanders (FWO-Vlaanderen)**
  - **Flemish Supercomputing Center (VSC)**

- **More information on *http//nele.studentenweb.org***

'Multiscale simulation of heterogeneous materials and coupling of thermodynamic models'
January 12-14, 2011

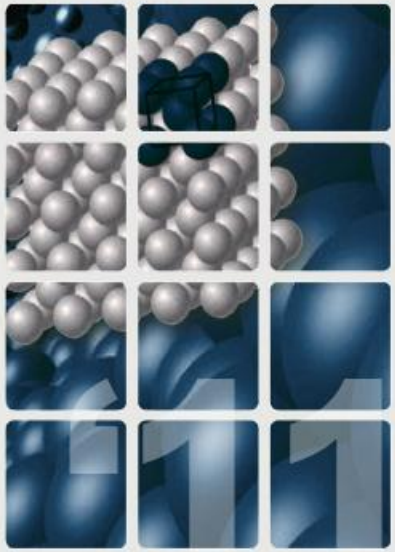

Home | Program | Registration | Venue | Sponsors | Contact

PROGRAM

Invited plenary speakers:

Mathematical multiscale techniques

Serge Prudhomme (Institute for Computational Engineering and Sciences, The University of Texas at Austin, USA)
Goal-oriented adaptivity for multiscale coupling methods

Mitchell Luskin (School of Mathematics, University of Minnesota, USA)
Accurate atomistic-to-continuum coupling methods for solids

Frederic Legoll (UR Navier, ENPC, Paris, France)
Finite temperature coarse-graining of atomistic models for solid materials

Marc Geers (Mechanical Engineering, Eindhoven University of Technology, the Netherlands)
Homogenization-based multi-scale computational solid mechanics: trends and challenges

Tim Schulze (Dept. of Mathematics, University of Tennesssee, USA)
Kinetic Monte Carlo simulation of heterostructured nanocrystalline growth

Aleksandar Donev (Courant Institute, New York University, USA)
Coarse-grained particle, continuum and hybrid models for complex fluids

Thermodynamic techniques/Alloys

Chris Wolverton (Dept. of Materials Science and Engineering, Northwestern University, USA)
TBA

Xavier Gonze (Institute of Condensed Matter and Nanoscience, Université Catholique de Louvain, Belgium)
First-principles computation of phonon spectra and thermodynamical properties

Carolyne Campbell (NIST/Metallurgy Division, USA)
Development of Multicomponent Diffusion Mobility Databases for Industrial Processing

Alan Dinsdale (COST MP0602) (National Physical Laboratory, Teddington, UK)
Computational thermodynamics and CALPHAD modeling for the development of high-temperature lead-free solder alloys

Ales Kroupa (COST MP0602) (Institute of Physics of Materials, Academy of Sciences of the Czech Republic)
COST MP0602 lead-free solder database: the design of a consistent thermodynamic database for complex multi-component alloys

Workshop on Multiscale simulation at K.U.Leuven

http://www.cs.kuleuven.be/conference/multiscale11/

KATHOLIEKE UNIVERSITEIT LEUVEN

thermo research group

Application examples

- **Coarsening of Al_6Mn precipitates located on a recrystallization front in Al-Mn alloys**

In collaboration with A. Miroux, E. Anselmino, S. van der Zwaag, T. U. Delft

Jerky motion during recrystallization in Al-Mn alloy

- In-situ EBSD observation of recrystallization in AA3103 at 400 °C
  - CamScan X500 Crystal Probe FEGSEM
- Jerky grain boundary motion
  - Stopping time: 15-25 s
  - Pinning by second-phase precipitates
    - $Al_6(Fe,Mn)$, α-$Al_{12}(Fe,Mn)_3Si$
- Added to phase field model
  - Grain boundary diffusion
  - Driving force for recrystallization

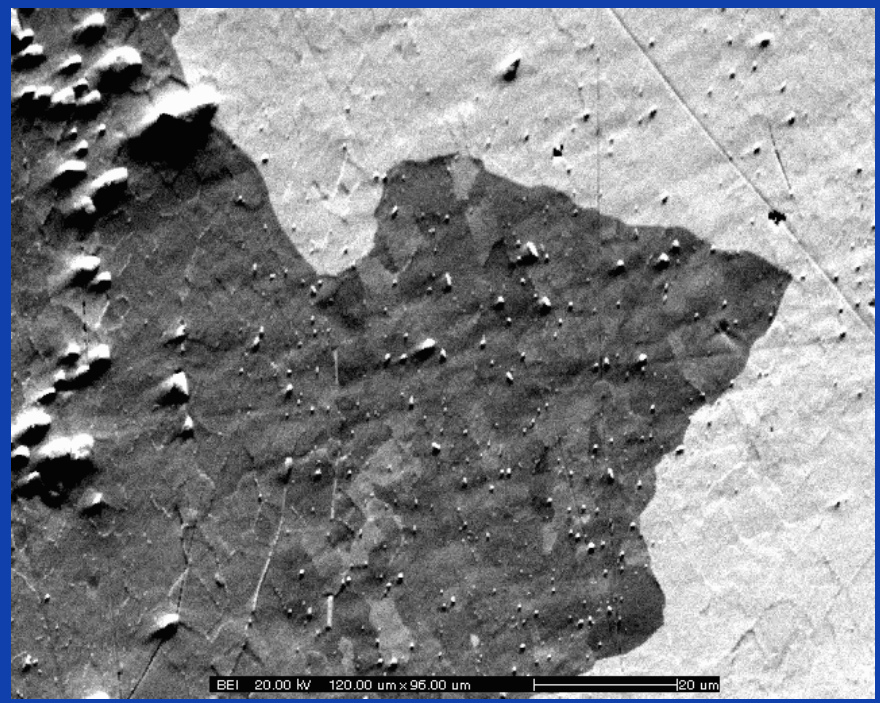

Phase field model

- **Multiple order parameter representation:** $\eta_{m,1}(\vec{r},t), \eta_{m,2}(\vec{r},t), \ldots, \eta_{p,i}(\vec{r},t), \ldots$

$$(\eta_{m,1}, \eta_{m,2}, \ldots, \eta_{p,i}, \ldots) = (1,0,\ldots,0,\ldots), (0,1,\ldots,0,\ldots), \ldots (0,0,\ldots,1,\ldots), \ldots$$

- **Mn composition field:** $x_{Mn}(\vec{r},t)$
- **Homogeneous driving pressure for recrystallization:** m_d
- **Bulk diffusion + Surface diffusion**

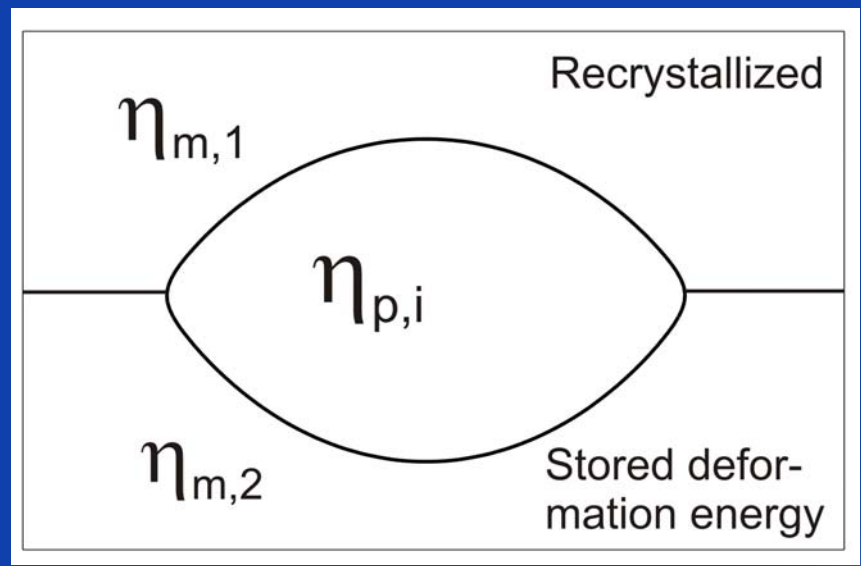

KATHOLIEKE UNIVERSITEIT LEUVEN

Material properties at 723K

Grain boundary energy high angle	γ_h = 0.324 J/m^2
Interfacial energy Al_6Mn precipitates	γ_{pr} = 0.3 J/m^2
Mobility high angle grain boundary At solute content 0.3w% Mn	$M_h = 2.94 \cdot 10^{-11}$ m^{2}s/kg (Miroux et al.,Mater. Sci. Forum,467-470,393(2004))
Equilibrium composition of matrix	$c_{Mn,eq}$ = 0.0524 w% (0.02456 at%) (PhD thesis Lok 2005)
Actual composition of matrix (supersaturated)	c_{Mn} = 0.3 w% (0.1474 at%) (PhD thesis Lok 2005)
Mn diffusion in fcc Al	$D_{0,bulk} = 10^{-2}$ m^2/s, Q_{bulk} = 211 kJ/mol $\rightarrow D_{bulk} = 5.5973 \cdot 10^{-18}$ m^2/s
Pipe diffusion high angle boundaries, precipitate/matrix interface	$D_{0,p} = D_{0,bulk}$, $Q_p = 0.65 Q_{bulk}$ $\rightarrow D_p = 1.2195 \cdot 10^{-12}$ m^2/s
Bulk energy density: $f^\rho = A^\rho(x-x^\rho_0)^2$	$A^m = 6 \cdot 10^{11}$; $x^m_0 = 0.000258$ $A^p = 6 \cdot 10^{12}$; $x^p_0 = 0.1429$

Precipitate coarsening and unpinning

- $P_D < P_{ZS}$ ($P_D \approx P_{ZS}$)
  - Pinning: P_{ZS}=3.6 MPa
  - Rex: P_D=3.1 MPa

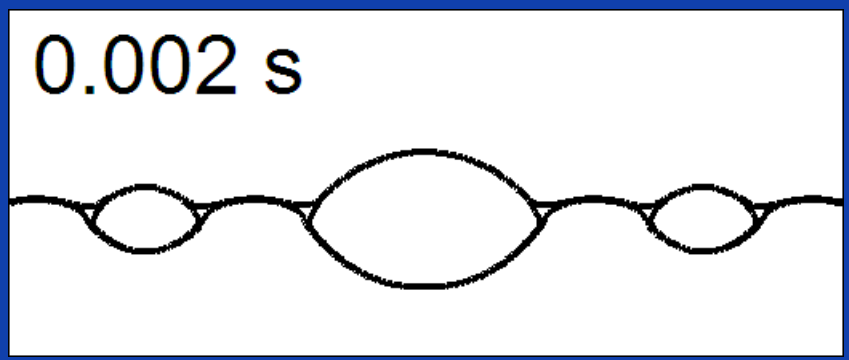

0.9μm *x* 0.375μm

- Unpinning mainly through surface diffusion around precipitates

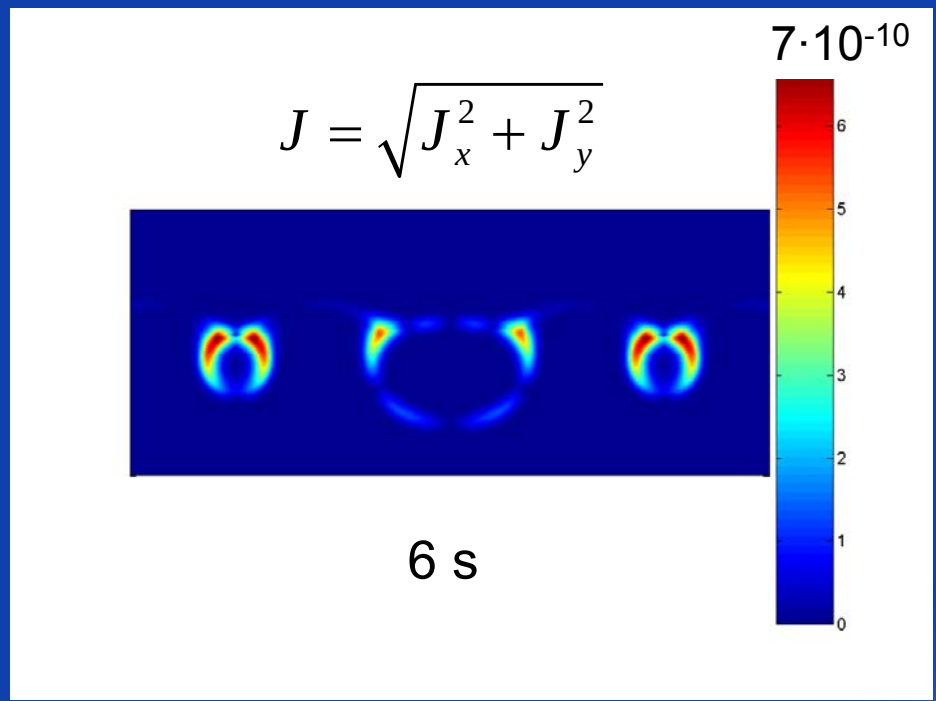

Precipitate coarsening and unpinning

- P_D <<< P_{ZS}
  - Pinning: P_{ZS} = 3.6 MPa
  - Rex: P_D = 1.1 MPa

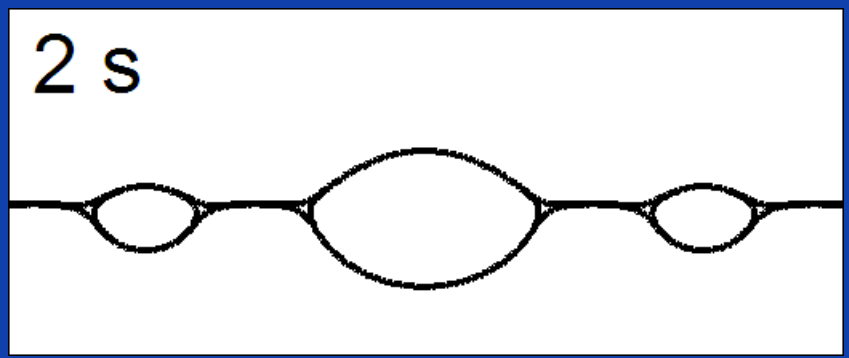

0.9μm *x* 0.375μm

- Unpinning through grain boundary diffusion

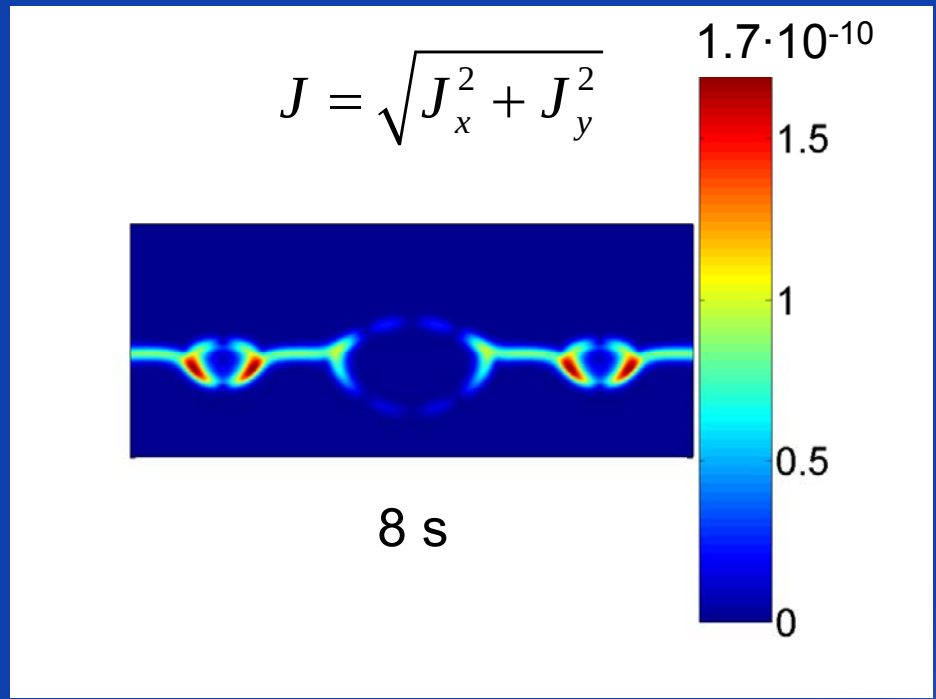

Multi-grain and multi-phase models

- **Multi-phase-field model**
  - **Phase fields** $\varphi_1, \varphi_2, \varphi_3, \ldots \varphi_p, \quad \sum_{i=1}^{p} \varphi_i = 1$
  - **Free energy** $f_{\text{int}} = \sum_{i \neq j} \frac{4\sigma_{i,j}}{\eta_{i,j}} \left\{ \frac{\eta_{i,j}^2}{\pi^2} |\nabla \phi_i \cdot \nabla \phi_j| + \phi_i \phi_j \right\}$ $\quad 0 < \phi_{i,j} < 1$
    - **Double obstacle, higher order terms, gradient term non-variational**
    - **Interpolation: zero-slope or thermodynamic consistency**

Steinbach et al.

MICRESS phase-field code

H. Garcke, B.Nestler, B. Stoth, SIAM J. Appl. Math. 60 (1999) p 295.

L.-Q. Chen and W. Yang, PRB, 50 (1994) p15752

- **Multi-order parameter models**
  - **Order parameters** $\eta_1, \eta_2, \ldots, \eta_i(\vec{r}, t), \ldots, \eta_p, \quad \left(\sum_{i=1}^{p} \eta_i \neq 1 \right)$
  - **Interfacial energy** $f_{\text{int}} = m \left(\sum_{i=1}^{p} \left(\frac{\eta_i^4}{4} - \frac{\eta_i^2}{2} \right) + \sum_{i=1}^{p} \sum_{j<i}^{p} \gamma_{i,j} \eta_i^2 \eta_j^2 + \frac{1}{4} \right) + \frac{\kappa(\eta)}{2} \sum_{i=1}^{p} (\vec{\nabla} \eta_i)^2$

A. Kazaryan et al., PRB, 61 (2000) p14275

KATHOLIEKE UNIVERSITEIT LEUVEN

Multi-grain and multi-phase models

- **Vector valued model**
  - **Orientation field (θ) and phase field (ϕ)**
  - **Free energy** $f_{\text{int}} = f(\phi, |\nabla\phi|, |\nabla\theta|)$

R. Kobayashi, J.A. Warren, W.C. Carter, Physica D, 119 (1998) p415

- **2-phase solidification**
  - **Phase fields** $\varphi_1, \varphi_2, \varphi_3, \quad \sum_{i=1}^{3} \varphi_i = 1$
  - **Fifth order interpolation functions $g_i(\phi_1,\phi_2,\phi_3)$**
    - **Zero-slope and thermodynamic consistent**
    - ***Order g_i* increases with number of phase-fields**

R. Folch and M. Plapp, PRE, 72 (2005) n° 011602

- **Multi-order parameter + 4th order gradient terms**

I.M. McKenna, M.P. Gururajan, P.W. Voorhees, J. Mater. Sci., 44 (2009) p2206

- **Phase field crystal and amplitude equations**

Rotation invariance of the model

- **Mathematically, the model equations are invariant to rotation, but …**
- **the order parameters represent orientations in a fixed reference frame.**

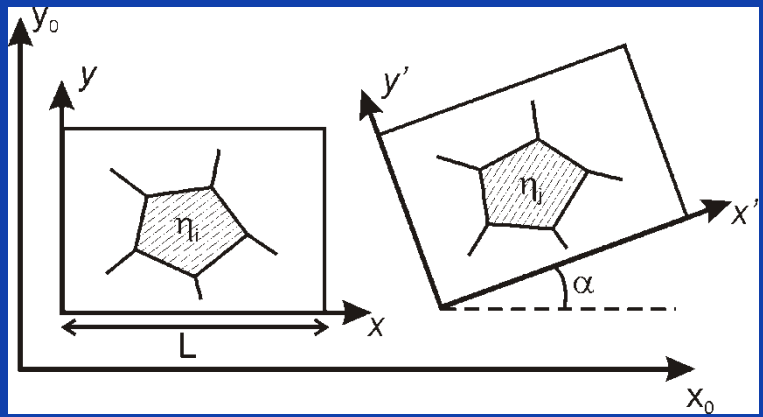

grid spacing Δh

physical width of domain L

rotational symmetry n

- **The precision of α depends on the numerical setup,**

$$\Delta\alpha \approx \frac{1}{\cos\alpha}\frac{\Delta h}{L}$$

- **For the model to be rotational invariant in practice, lower limit of amount of order parameters p:**

$$p > \frac{\sqrt{2}\pi L}{n\Delta h}$$

J. Heulens and N. Moelans, Scripta Mat. (2010)